Exact algorithm for d-dimensional walks on finite and infinite lattices with traps. III. Role of lattice valency in influencing the efficiency of diffusion-controlled reactions

Philip A. Politowicz and John J. Kozak
Department of Chemistry and Radiation Laboratory, University of Notre Dame, Notre Dame, Indiana 46556
(Received 13 January 1983; revised manuscript received 15 July 1983)

In this paper we continue our development of an exact lattice theory of diffusion-controlled reactions. We show how general theorems drawn from the theory of finite Markov processes may be brought to bear on the approach elaborated in our earlier work [Phys. Rev. Lett. 47, 1500 (1981); Phys. Rev. B 26, 4166 (1982)] and, in addition, we exploit well-known diagram and generating-function methods (in particular, those based on the adjacency-walk matrix) to gain further insight into the statistics underlying the processes considered in this paper. We consider reactions in which the diffusing molecule encounters a single reaction center and reacts there, irreversibly, upon first encounter. We also consider the situation where the diffusing particle may, at any of the sites surrounding the reaction center, form an activated complex with a coreactant situated there and, with finite probability, be removed irreversibly from the system. In each case we focus on the problem of reaction efficiency and determine the average number of steps required before a diffusing particle undergoes, eventually, an irreversible reaction. We report extensive new (and *exact*) results for hexagonal lattices and consider explicitly the role of spatial extent and dimensionality as well as the influence of passive versus active boundary conditions. By comparing the results obtained for hexagonal lattices for $d=2$ and 3 with those reported earlier for square and/or cubic lattices, quantitative conclusions can be drawn on the role of lattice valency in influencing the efficiency of reaction-diffusion processes. A principal, general conclusion of this study concerns the efficiency of reaction when there exists the possibility of reactant deactivation at the $N-1$ sites surrounding the reaction center. We find that a 5% probability of reaction at these adjacent sites effectively erases distinctions between lattices subject to different boundary conditions or characterized by different valencies, i.e., the process becomes kinetically controlled.

I. INTRODUCTION

In this paper we exploit the fact that the theory of random walks on lattices with traps provides a valuable theoretical framework for studying the factors which influence diffusion-controlled reactions in heterogeneous, (e.g., compartmentalized) and homogeneous (extended) systems. Although several problems involving random walks on lattices decorated with traps are susceptible to analysis using the method of generating functions, each new result here (especially for dimensions other than $d=1$ and for boundary conditions other than periodic) has usually necessitated a tour de force of mathematical physics.[1-3] Alternatively, concrete results for reaction-diffusion processes in d dimensions and for a wide class of boundary conditions can be obtained via straightforward Monte Carlo simulation.[4-6] Here, however, the central processing unit (CPU) times required for carrying through such computations and obtaining reliable estimates of the average walk length escalate rapidly once more than a few hundred lattice sites are considered. Intermediate between the two strategies noted above is the procedure introduced in Refs. 7 and 8 (hereafter referred to as I and II, respectively) wherein d-dimensional walks on finite and infinite lattices with traps were studied and quantified using an exact algorithm. Implementation of this algorithm allowed the calculation of exact results for a wide variety of lattice problems previously resistant to exact or asymptotic analysis; moreover, these results could be generated numerically on time scales essentially negligible with respect to those required for the corresponding Monte Carlo simulation. In fact, especially in II, we have stressed that the plethora of exact numerical results that can be generated using the algorithm provides, in effect, a bank of experimental evidence that can be used to guide the development of analytic theories of lattice statistical problems; some progress along these lines was reported in II.

The objectives of the present contribution are threefold. Firstly, we wish to establish the relationship between the classical theory of finite Markov processes and the algorithm reported in I and II; in so doing, we shall place the approach laid down in I and II within the context of a general theory, further aspects of which can then be exploited to study a variety of problems in reaction-diffusion theory. Secondly, we shall use diagram and generating function methods (specifically those based on the adjacency-walk matrix) in conjunction with Markov-chain results to gain insights into the statistical probabilities governing site encounters in reaction-diffusion processes. Finally, we shall take up the specific problem of lattice valency and determine the extent to which this characteristic feature of a lattice system influences the efficiency of diffusion-controlled chemical processes. To quantify our analysis of valency, we shall provide a reasonably complete description of reaction-diffusion processes on hexagonal lattices, focusing on the role of dimensionality, spatial extent, and the influence of boundary conditions. By comparing the results obtained with our earlier studies

on square and/or cubic lattices, the interplay between lattice valency and the above variables in determining the efficiency of reaction-diffusion processes can be studied and the relative importance of these factors assessed.

The plan of this paper is the following. In Sec. II we review our approach to the problem of reaction-diffusion processes on d-dimensional lattices, and illustrate for hexagonal lattices how the problem may be formulated and the calculation of average walk lengths simplified by taking maximal advantage of the point symmetry of the underlying lattice. By drawing on known theorems from the theory of finite Markov processes,[9] we then establish the rigorous mathematical basis for the results obtained in our calculations, and thereby give a clearer picture of the factors which influence reaction-diffusion processes in latticelike systems. In that section as well we mobilize diagram methods[10] to construct the adjacency-walk matrix for the hexagonal lattices studied in this paper. The results obtained here cast light (we believe) on the statistical factors involved in constructing purely numerical (Monte Carlo) estimates of the efficiency of trapping on decorated lattices. Reasonably comprehensive results for two classes of reaction-diffusion processes on hexagonal lattices are presented in Sec. III and comparisons of trapping efficiency in hexagonal versus square and/or cubic lattice systems are presented and discussed in Sec. IV. Although representative results are given for the dimensionality $d=3$, the primary emphasis in our assessment of the role of lattice valency will be on two-dimensional systems since, in our formulation, hexagonal and square lattices can be placed in exact correspondence, and the conclusions drawn are therefore unequivocal.

II. THEORETICAL BACKGROUND

A. Identification of the unit cell (simplex)

Consider a plane ($d=2$) covered with a number of contiguous regular hexagons. We regard the sites visited by a randomly moving, diffusing particle to be the vertices of this array of hexagons with the sides of each hexagon representing possible paths between sites of the lattice. A sketch of such an array is given in Fig. 1, where the circles indicate the lattice sites (vertices). Note the triangular dashed boundary in the center of the figure. It is evident that the entire lattice section displayed could be constructed by juxtaposing a number of such triangular units (simplexes), a consequence of the fact that the dual lattice of a hexagonal system is a triangular lattice. By building outward from a centrally positioned (irreducible) triangular unit with a centrosymmetric trap, extended triangular networks are obtained which have a number N of sites equal to the square of an integer. Such a construction has two principal advantages. Since N is the square of an integer, we shall later (Sec. IV) be able to compare directly results obtained for hexagonal lattices with those reported previously for square lattices (in II); there, our objective will be to determine how the efficiency of reaction-diffusion processes depends on the valency ν of the lattice assumed ($\nu=d+1$ for hexagonal lattices and $\nu=2d$ for square and/or cubic lattices). Secondly, the results generated for a lattice with a centrosymmetric trap are identical for two

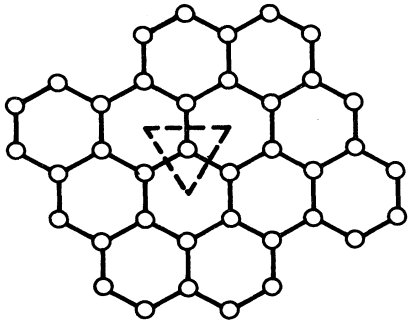

FIG. 1. Diagram of a portion of the general, $d=2$ hexagonal lattice. Circles (vertices) indicate lattice sites and connecting lines (bonds) indicate the paths accessible to the diffusing particle. Dashed triangle defines the basic irreducible unit of the associated dual lattice.

important classes of boundary conditions: periodic boundary conditions and nontransmitting boundary conditions, the latter boundary conditions serving to confine the walker to a finite region of space.

The specifications noted above eliminate certain units generated from a triangular unit cell. The first three hexagonal lattices that satisfy the specifications have $N=1$, 4, and 16 sites, the latter being the first mathematically interesting case (see Fig. 2). The case $N=16$ will now be used to illustrate the classification of the (point) symmetry of the lattice.

B. Classification of the point symmetry

For definiteness we consider the centrosymmetric site to be a trap T and we organize the $N-1$ remaining sites of the lattice with respect to this site. By inspection, one notices that the triangular unit diagrammed in Figs. 2 and 3 has three C_2 (twofold) axes in the plane of the unit and a C_3 (threefold) axis perpendicular to that plane and passing through the trap T. Using these symmetry elements, one can distinguish sites of the same symmetry as one moves radially outward from the central site T. Sites of similar

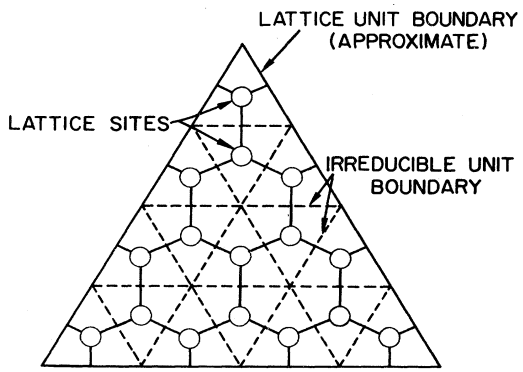

FIG. 2. Construction of the smallest $d=2$ hexagonal unit considered in this paper. Irreducible triangular lattice units are juxtaposed to form the $N=16$ hexagonal lattice.

symmetry are labeled by positive integers. An example of a site-classified unit is displayed in Fig. 3. Again by inspection one finds that the numerically labeled sites of Fig. 3 are of two (and only two) distinct multiplicities, viz., multiplicity 3 or multiplicity 6, with sites of multiplicity 3 greater in number. Later we will find that the imposition of certain boundary conditions can reduce the symmetry of the lattice; effectively, sites of multiplicity 6 are replaced by sites of multiplicity equal to or less than 3.

The great practical advantage of the symmetry classification scheme introduced above is that, with respect to the eventual computations to be performed, the scheme reduces significantly the number of independent variables (and hence the number of equations) to be considered. For example, in the case diagrammed in Fig. 3, the number of lattice sites that have to be dealt with explicitly in the calculations collapses from 16 to 5. The site classification scheme for the unit $N=25$ is shown in Fig. 4. The same basic symmetry classification schemes were implemented for all the hexagonal lattices considered in this paper (e.g., for $d=2$, up to $N=361$). The diagrams presenting the classifications for all the units considered for the case of periodic and nontransmitting boundary conditions are displayed in Figs. 5(a) and 5(b), with the site specifications of the smaller units studied forming subsets of the site specifications of the largest units, $N=289$ and 361.

C. Boundary conditions

A further rationale for the classification scheme described in the two preceding subsections is that, as can be seen in Fig. 3, every walker's path leading out of or into the lattice unit is perpendicular to the boundary. This feature also characterizes the possible exit-reentry trajectories on square lattices, as can be seen from the diagrams presented in II. The chief advantage of this construction is that the identification and characterization of a variety of boundary conditions then becomes a straightforward and systematic task. For example, to generate periodic boundary conditions for any of the triangular "unit cells," one simply places three identical lattice units against the faces of the original lattice unit. With the use of this scheme, if a random walker were on the site "2" marked by an asterisk in Fig. 3, a step taken across the face of the original lattice unit would put the walker at another site labeled 2 on an adjacent unit (since all three faces of the original lattice unit are identical with respect to sites adjacent to the boundary). Consider next the vertex site "4" marked with an asterisk in Fig. 3; a random walker stepping *either* way off this vertex site would wind up at a site 4 on one of the juxtaposed lattices. Therefore, given the construction of the basic simplex and the (point-) group classification of the sites of the lattice described above, one is led to a natural identification of periodic boundary conditions for the problem at hand. Inasmuch as we have specified the trap T to be centrosymmetric, the fate of the random walker would be the same if it were to have confronted nontransmitting (or confining) boundary conditions. That is, suppose the walker were positioned at a site labeled 2 in Fig. 3; if the lattice were assumed to be *finite* and subject to nontransmitting boundary conditions,

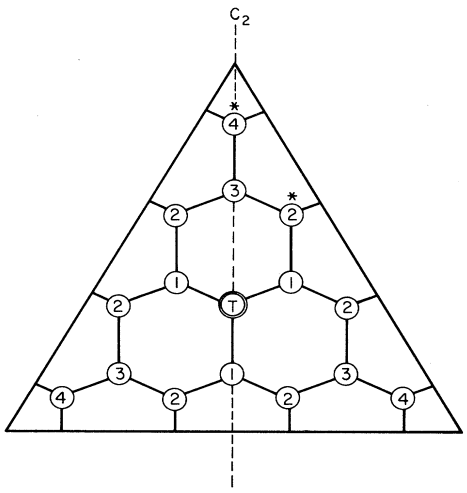

FIG. 3. Hexagonal lattice unit of Fig. 2 subject to periodic boundary conditions with the centrosymmetric trap T and the site classifications of the $N-1$ neighboring sites indicated explicitly. Sites marked with an asterisk are referred to in the text.

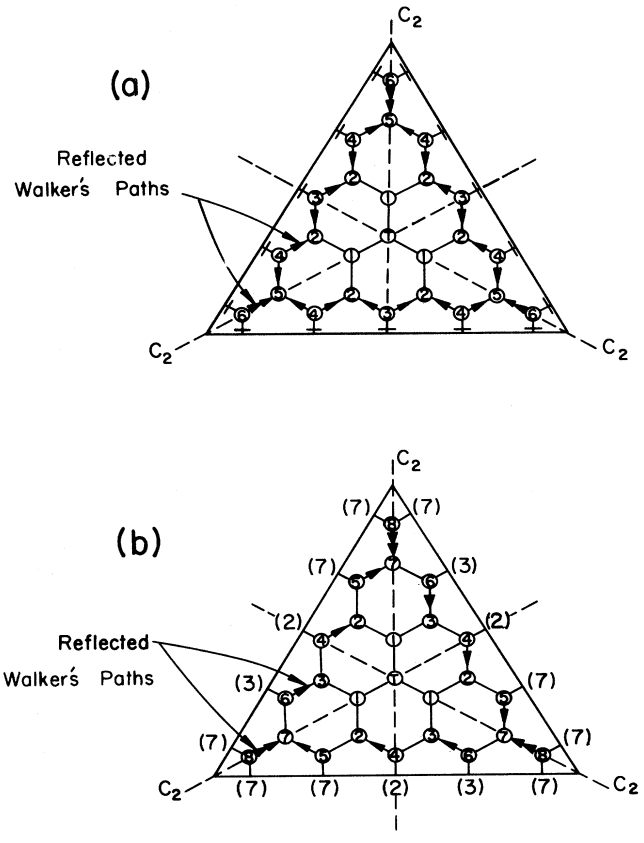

FIG. 4. (a) Site classification for the hexagonal lattice unit with $N=25$ subject to reflecting boundary conditions with the equal-probability convention assumed. (b) Site classification for the hexagonal lattice unit with $N=25$ subject to reflecting boundary conditions with the clockwise-bias convention assumed.

an attempt by the walker to step across the boundary would result in the walker's being reset at the position 2, thereby leading to the same net result as was described for the case of periodic boundary conditions.

From the above description it is seen that both periodic and nontransmitting or confining boundary conditions are essentially passive boundary conditions and that both situations have a direct correspondence, in terms of their formulation and interpretation, to boundary conditions imposed on square and/or cubic lattices in d dimensions. However, one encounters a fundamentally new situation *vís a vís* square lattices if one permits the boundary to influence "actively" the trajectory of the random walker. The simplest new situation involves the case of reflecting boundary conditions. For the case of square lattices subject to reflecting boundary conditions, a walker attempting to step off the lattice (or to step across the boundary) is reflected back into the lattice to the next interior site along a path perpendicular to the unit lattice boundary. For hexagonal lattices there is no path perpendicular to the unit lattice boundary and directed into the unit lattice. Instead, upon reflection at the boundary (at least) two fates are possible for the random walker. For definiteness, consider the random walker moving from the site labeled 2 and marked with an asterisk in Fig. 3 toward the boundary. The simplest possibility upon reflection at the boundary would be that the walker moves to sites "1" or "3" with equal *a priori* probabilities. For a walker starting from the vertex site 4, traversing either outward trajectory would result in the walker's being reflected upon confronting the boundary to the site labeled 3 adjacent to the original site 4. We shall refer to this specification for reflecting boundary conditions (RBC's) at border and vertex sites as defining the equal-probability convention for RBC's; in this scenario, the fate of the random walker is inherently the most "random" upon confronting the reflecting boundary. Figure 4(a) shows how this convention would distribute reflected walker's paths over the entire lattice unit.

Given reflection at a boundary, one might also imagine that a bias has been imposed on the reflected walker's motion upon encountering the boundary. For example, a walker at the marked site 2 in Fig. 3 might be reflected always to the site labeled 1 upon hitting the boundary, i.e., its reflection would be biased in a clockwise direction. If such a bias is systematically applied to the other border lattice sites then, for example, a walker at the site marked 2 on the other (vertical) leg of the unit lattice would be reflected to the site 3 (up the page in Fig. 3). A walker at a vertex site 4 would still be reflected to an adjacent internal site 3. The net consequence of applying reflecting boundary conditions with the clockwise-bias convention is that sites of multiplicity 6 become unequivalent and, in fact, become two sites, each of multiplicity 3. Thus, to study the reaction-diffusion problem generated when a diffusing particle encounters a reflecting boundary and is biased in the path it takes upon reentering the lattice, one must first reclassify the sites of the unit lattice. The procedure for doing so is straightforward and simply leads to an increase in the total number of lattice sites (and hence equations) that must be considered explicitly [see Fig. 4(b)].

It is clear from the above discussion (and the one immediately following) that a whole class of boundary conditions on hexagonal (and square and/or cubic) lattices might be designed and easily implemented. Since our principal goal in this paper is to assess the role of lattice valency ν in influencing the efficiency of reaction-diffusion processes, the calculations reported later (in Sec. III) on periodic, nontransmitting [see Figs. 5(a) and 5(b)] or reflecting [see Figs. 6(a) and 6(b)] boundary conditions (the latter assuming the equal-probability convention and the clockwise-bias convention) will be taken as representative of the sorts of effects one finds upon imposing passive versus active boundary conditions.

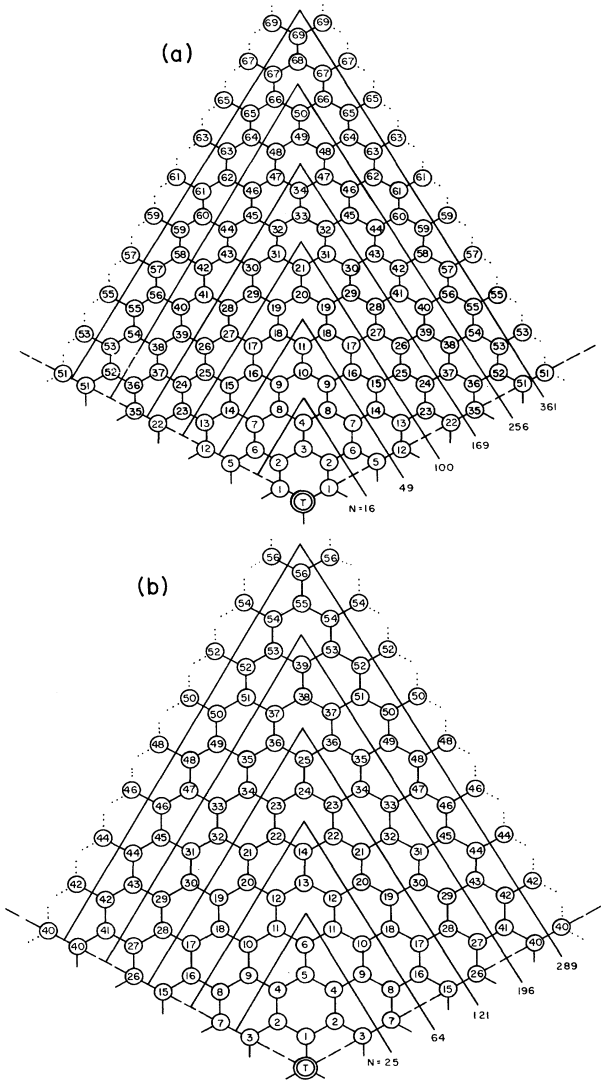

FIG. 5. (a) Site classifications for hexagonal lattice units with $N=16$, 49, 100, 169, 256, and 361, subject to periodic or confining boundary conditions. This site classification scheme, and that shown in (b), also applies to lattice units subject to reflecting boundary conditions using the equal-probability convention. (b) Site classifications for hexagonal lattice units with $N=25$, 64, 121, 196, and 289, subject to periodic or confining boundary conditions.

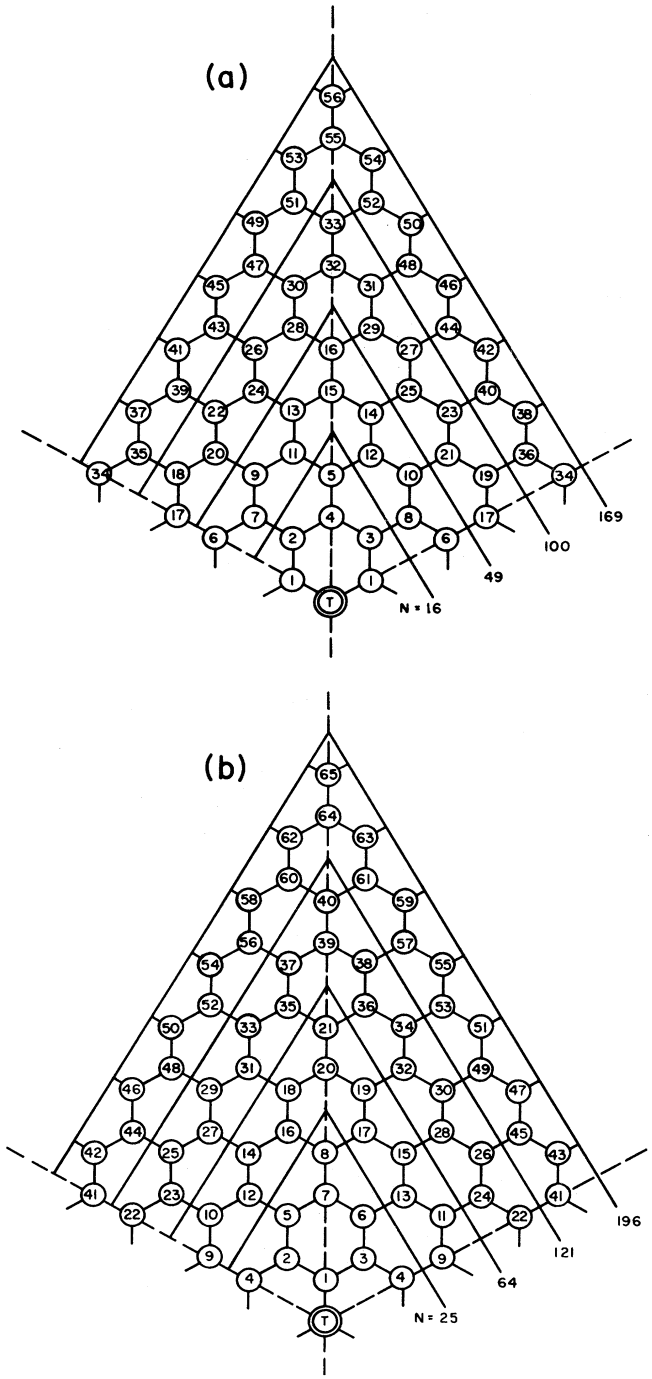

FIG. 6. (a) Site classifications for hexagonal lattice units with $N=16$, 49, 100, and 169, subject to reflecting boundary conditions using the clockwise-bias convention. (b) Site classifications for hexagonal lattice units with $N=25$, 64, 121, and 196, subject to reflecting boundary conditions using the clockwise-bias convention.

D. Determination of the average walk length

To set the present study (and the earlier studies I and II) within the framework of the canonical theory of finite Markov processes, we demonstrate first the construction of the transformation matrix for the class of reaction-diffusion problems considered here. Consider the lattice unit of Fig. 3 under the influence of periodic boundary conditions. Subject to these boundary conditions, when a random walker attempts to step off the unit lattice, it lands on a site whose symmetry classification is identical to the one it just left. Thus, for example, consider a walker positioned on site 1. The walker will have arrived at site 1 from one of three possible sites: the site labeled T or either of the two sites labeled 2. When equal *a priori* probabilities govern the motion of the random walker, the attendant probability is just the reciprocal of the lattice valency: in Fig. 3, $\nu=3$ and the probability $p_{i\to j}=\frac{1}{3}$ for $i\neq j$. Now, let us assume that the walks *to* site 1 from the site T or from either of the sites 2 were realized with equal *a priori* probabilities and that except for these one-step events the walker has lost all memory of the previous history of the sites traversed. Then, in this Markovian scenario, the average walk length $\langle n\rangle_1$ *from* site 1 will be

$$\langle n\rangle_1=\tfrac{1}{3}(\langle n\rangle_T+1)+\tfrac{1}{3}(\langle n\rangle_2+1)+\tfrac{1}{3}(\langle n\rangle_2+1)\,, \tag{1}$$

i.e., one step plus the average walk length $\langle n\rangle_T$ from site T, with the sum weighted by the probability ($\frac{1}{3}$) of having arrived at site 1 from T; a similar description pertains for nearest-neighbor walks from the sites 2. By inspection of Fig. 3, the average walk lengths from each of the remaining sites of the unit lattice may be written similarly as

$$\langle n\rangle_T=\tfrac{1}{3}(\langle n_1\rangle+1)+\tfrac{1}{3}(\langle n\rangle_1+1)+\tfrac{1}{3}(\langle n\rangle_1+1)\,, \tag{2}$$

$$\langle n\rangle_2=\tfrac{1}{3}(\langle n\rangle_1+1)+\tfrac{1}{3}(\langle n\rangle_2+1)+\tfrac{1}{3}(\langle n\rangle_3+1)\,, \tag{3}$$

$$\langle n\rangle_3=\tfrac{1}{3}(\langle n\rangle_2+1)+\tfrac{1}{3}(\langle n\rangle_2+1)+\tfrac{1}{3}(\langle n\rangle_4+1)\,, \tag{4}$$

$$\langle n\rangle_4=\tfrac{1}{3}(\langle n\rangle_3+1)+\tfrac{1}{3}(\langle n\rangle_4+1)+\tfrac{1}{3}(\langle n\rangle_4+1)\,. \tag{5}$$

The system of five equations, Eqs. (1)—(5), in five unknowns may be solved directly via Cramer's rule to obtain explicit expressions for the unknowns: $\langle n\rangle_T$, $\langle n\rangle_1$, $\langle n\rangle_2$, $\langle n\rangle_3$, and $\langle n\rangle_4$. From this determination the overall average walk length $\langle n\rangle$ may be computed from the expression

$$\langle n\rangle=\frac{\langle n\rangle_T+3\langle n\rangle_1+6\langle n\rangle_2+3\langle n\rangle_3+3\langle n\rangle_4}{N-1}\,. \tag{6}$$

Thus, the straightforward, self-consistent characterization of the (mean) fate of a random walker as it confronts a site of given symmetry on a lattice leads at once to an expression for the overall walk length $\langle n\rangle$. If it happens that the centrosymmetric site T is a deep trap, so that upon stepping on the site T the walker is irreversibly removed from the stochastic process (in which case the probability of being trapped at the site T is $p_T=1$), then the average walk length *from* site T is

$$\langle n\rangle_T=0\,. \tag{7}$$

The expression for $\langle n\rangle_1$ becomes

$$\langle n\rangle_1=1+\tfrac{2}{3}\langle n\rangle_2\,, \tag{8}$$

with the remaining equations [Eqs. (3)—(5)] for $\langle n\rangle_2$, $\langle n\rangle_3$, and $\langle n\rangle_4$ the same; $\langle n\rangle$ is then computed from Eq. (6), upon incorporating the modifications, Eqs. (7) and (8).

For the problem described above one can also organize the information describing the diffusing particle's walk through the lattice in a matrix representation. When the site T is a passive (neutral) site, i.e., not a deep trap, the relevant matrix [constructed from Eqs. (1)—(5)] is

$$\begin{bmatrix} 1 & -1 & 0 & 0 & 0 \\ -\frac{1}{3} & 1 & -\frac{2}{3} & 0 & 0 \\ 0 & -\frac{1}{3} & +\frac{2}{3} & -\frac{1}{3} & 0 \\ 0 & 0 & -\frac{2}{3} & 1 & -\frac{1}{3} \\ 0 & 0 & 0 & -\frac{1}{3} & +\frac{1}{3} \end{bmatrix} \begin{bmatrix} \langle n \rangle_T \\ \langle n \rangle_1 \\ \langle n \rangle_2 \\ \langle n \rangle_3 \\ \langle n \rangle_4 \end{bmatrix} = \begin{bmatrix} 1 \\ 1 \\ 1 \\ 1 \\ 1 \end{bmatrix} . \tag{9}$$

If the site T is a deep trap, we have, from Eqs. (3)—(5), (7), and (8),

$$\begin{bmatrix} 1 & 0 & 0 & 0 & 0 \\ -\frac{1}{3} & 1 & -\frac{2}{3} & 0 & 0 \\ 0 & -\frac{1}{3} & +\frac{2}{3} & -\frac{1}{3} & 0 \\ 0 & 0 & -\frac{2}{3} & 1 & -\frac{1}{3} \\ 0 & 0 & 0 & -\frac{1}{3} & +\frac{1}{3} \end{bmatrix} \begin{bmatrix} \langle n \rangle_T \\ \langle n \rangle_1 \\ \langle n \rangle_2 \\ \langle n \rangle_3 \\ \langle n \rangle_4 \end{bmatrix} = \begin{bmatrix} 0 \\ 1 \\ 1 \\ 1 \\ 1 \end{bmatrix} . \tag{10}$$

For future reference, let us define the 5×5 matrix appearing on the left-hand side of Eq. (10) as $\underline{\tilde{A}}$; the 4×4 submatrix appearing in the lower right-hand corner of this last equation will be defined as

$$\begin{bmatrix} 1 & -\frac{2}{3} & 0 & 0 \\ -\frac{1}{3} & +\frac{2}{3} & -\frac{1}{3} & 0 \\ 0 & -\frac{2}{3} & 1 & -\frac{1}{3} \\ 0 & 0 & -\frac{1}{3} & +\frac{1}{3} \end{bmatrix} \equiv \underline{A} . \tag{11}$$

The lattice model described above, with T a deep trap, is a paradigm for an important class of reaction-diffusion processes, viz., reactions in which the diffusing molecule encounters a single reaction center and reacts there, irreversibly, upon first encounter. We should also like to consider processes where the diffusing particle may, at any of the sites surrounding the reaction center, form an activated complex with a coreactant situated there and, with finite probability, be removed irreversibly from the system. To develop a lattice model for this situation, we regard the centrosymmetric site T to be characterized by an absorption probability p_T (with $0<p_T\leq1$) with each of the $N-1$ remaining sites i to be characterized by an absorption probability s_i (with $0<s_i\leq1$). Although the general case, $s_i\neq s_j$ for all i,j, is certainly of interest and could be treated by the methods described above, in this paper we shall assume that all $s_i=s$, i.e., we assume a uniform probability of reaction at each of the $N-1$ neighboring sites. Since the probability that a walker is *not* trapped at one of these $N-1$ sites is $1-s$, the equations [Eqs. (1)—(5)] listed above may be generalized to deal with the competitive trapping situation by multiplying each factor on the right-hand side of each by the factor $1-s$ and complementing each equation by the further factor, $s(1)$, the probability of the walker being trapped at the auxiliary site in question. These modifications result in the following set of equations:

$$\langle n \rangle_T = p_T(1)+(1-p_T)[(\langle n \rangle_1+1)] , \tag{12}$$

$$\langle n \rangle_1 = s(1)+(1-s)[\tfrac{1}{3}(\langle n \rangle_T+1)+\tfrac{2}{3}(\langle n \rangle_2+1)] , \tag{13}$$

$$\langle n \rangle_2 = s(1)+(1-s)[\tfrac{1}{3}(\langle n \rangle_1+1)+\tfrac{1}{3}(\langle n \rangle_2+1) + \tfrac{1}{3}(\langle n \rangle_3+1)] , \tag{14}$$

$$\langle n \rangle_3 = s(1)+(1-s)[\tfrac{2}{3}(\langle n \rangle_2+1)+\tfrac{1}{3}(\langle n \rangle_4+1)] , \tag{15}$$

$$\langle n \rangle_4 = s(1)+(1-s)[\tfrac{1}{3}(\langle n \rangle_3+1)+\tfrac{2}{3}(\langle n \rangle_4+1)] . \tag{16}$$

The corresponding transformation matrix is

$$\begin{bmatrix} 1 & -t & 0 & 0 & 0 \\ -q & 1 & -2q & 0 & 0 \\ 0 & -q & 1-q & -q & 0 \\ 0 & 0 & -2q & 1 & -q \\ 0 & 0 & 0 & -q & 1-2q \end{bmatrix} \begin{bmatrix} \langle n \rangle_T \\ \langle n \rangle_1 \\ \langle n \rangle_2 \\ \langle n \rangle_3 \\ \langle n \rangle_4 \end{bmatrix} = \begin{bmatrix} 1 \\ 1 \\ 1 \\ 1 \\ 1 \end{bmatrix} , \tag{17}$$

where we have set $q=\frac{1}{3}(1-s)$ and $t=1-p_T$. If it is assumed that reaction at site T is strictly irreversible, i.e., T is a deep trap and the average number of steps required for trapping starting *from* site T is $\langle n \rangle_T=0$, then the above matrix equation simplifies to

$$\begin{bmatrix} 1 & 0 & 0 & 0 & 0 \\ -q & 1 & -2q & 0 & 0 \\ 0 & -q & 1-q & -q & 0 \\ 0 & 0 & -2q & 1 & -q \\ 0 & 0 & 0 & -q & 1-2q \end{bmatrix} \begin{bmatrix} \langle n \rangle_T \\ \langle n \rangle_1 \\ \langle n \rangle_2 \\ \langle n \rangle_3 \\ \langle n \rangle_4 \end{bmatrix} = \begin{bmatrix} 0 \\ 1 \\ 1 \\ 1 \\ 1 \end{bmatrix} . \tag{18}$$

E. Connection with the theory of finite Markov processes

The formulation presented in the preceding sections is based on a self-consistent coding of the fate of a particle diffusing on a lattice of valency ν and dimensionality d, and encountering there sites of given symmetry and reactivity. We now establish the relationship between this formulation and the theory of finite Markov processes. In so doing, by virtue of theorems already available from the theory of Markov processes, we will place the interpretation of our numerical results on a sound theoretical footing. Conversely, the extensive numerical results obtained via implementation of the program described in I, II, and in Secs. II A—II C, provide a bank of experimental evidence which may be used to guide the construction of new theorems and estimates in Markov chain theory.

To assist the reader in our development, in the discussion we shall refer to the standard text of Kemeny and Snell[9] for definitions and relevant theorems. We shall consistently use their notation, *except* that their Roman symbols will systematically be replaced by script letters to avoid confusion with other parts of this paper. The definitions and theorems cited below will be designated as in Ref. 9.

Central to the formulation of Markov chain theory is the identification of probabilities $\mathcal{P}_{ij}$ and the construction of a transition matrix $\underline{\mathcal{P}}$. Given a conditional probability $\Pr[\mathcal{q} \mid \mathcal{r}]$, where $\mathcal{r}$ and $\mathcal{q}$ are statements which are independent and neither a self-contradiction, the n-step transition probabilities for a Markov process, denoted by $\mathcal{P}_{ij}(n)$ are (Definition 2.1.2 of Ref. 9)

$$\mathcal{P}_{ij}(n)=\Pr[\mathcal{f}_n=\mathcal{s}_j \mid \mathcal{f}_{n-1}=\mathcal{s}_i] . \tag{19}$$

Here, the $\mathcal{f}_n$ is the outcome function, the value of which is $\mathcal{s}_j$ if the outcome of the nth experiment is $\mathcal{s}_j$. A finite Markov process is a finite Markov chain if the transition probabilities $\mathcal{P}_{ij}(n)$ do not depend on n (Definition 2.1.3). Then, the transition matrix $\underline{\mathcal{P}}$ for a Markov chain is the matrix $\underline{\mathcal{P}}$ with entries $\mathcal{P}_{ij}$.

Let us now write down the matrix $\underline{\mathcal{P}}$ corresponding to the problem summarized by Eqs. (1)–(5). Here we consider all possible transitions between sites $\mathcal{s}_i$ of the lattice diagrammed in Fig. 3 (subject to periodic boundary conditions) and specified by the attendant probabilities $\mathcal{P}_{ij}$ of the process $\mathcal{s}_i \to \mathcal{s}_j$. That is, we construct

$$\underline{\mathcal{P}}=\begin{array}{c} \\ \mathcal{s}_T \\ \mathcal{s}_1 \\ \mathcal{s}_2 \\ \mathcal{s}_3 \\ \mathcal{s}_4 \end{array}\begin{array}{c} \begin{array}{ccccc} \mathcal{s}_T & \mathcal{s}_1 & \mathcal{s}_2 & \mathcal{s}_3 & \mathcal{s}_4 \end{array} \\ \begin{pmatrix} \mathcal{s}_T\to\mathcal{s}_T & \mathcal{s}_T\to\mathcal{s}_1 & \mathcal{s}_T\to\mathcal{s}_2 & \mathcal{s}_T\to\mathcal{s}_3 & \mathcal{s}_T\to\mathcal{s}_4 \\ \mathcal{s}_1\to\mathcal{s}_T & \mathcal{s}_1\to\mathcal{s}_1 & \mathcal{s}_1\to\mathcal{s}_2 & \mathcal{s}_1\to\mathcal{s}_3 & \mathcal{s}_1\to\mathcal{s}_4 \\ \mathcal{s}_2\to\mathcal{s}_T & \mathcal{s}_2\to\mathcal{s}_1 & \mathcal{s}_2\to\mathcal{s}_2 & \mathcal{s}_2\to\mathcal{s}_3 & \mathcal{s}_2\to\mathcal{s}_4 \\ \mathcal{s}_3\to\mathcal{s}_T & \mathcal{s}_3\to\mathcal{s}_1 & \mathcal{s}_3\to\mathcal{s}_2 & \mathcal{s}_3\to\mathcal{s}_3 & \mathcal{s}_3\to\mathcal{s}_4 \\ \mathcal{s}_4\to\mathcal{s}_T & \mathcal{s}_4\to\mathcal{s}_1 & \mathcal{s}_4\to\mathcal{s}_2 & \mathcal{s}_4\to\mathcal{s}_3 & \mathcal{s}_4\to\mathcal{s}_4 \end{pmatrix} \end{array} . \tag{20}$$

For the case in which the centrosymmetric site T is not a deep trap, the transition matrix $\underline{\mathcal{P}}$ reads

$$\underline{\mathcal{P}}=\begin{array}{c} \\ \mathcal{s}_T \\ \mathcal{s}_1 \\ \mathcal{s}_2 \\ \mathcal{s}_3 \\ \mathcal{s}_4 \end{array}\begin{array}{c} \begin{array}{ccccc} \mathcal{s}_T & \mathcal{s}_1 & \mathcal{s}_2 & \mathcal{s}_3 & \mathcal{s}_4 \end{array} \\ \begin{pmatrix} 0 & +1 & 0 & 0 & 0 \\ +\frac{1}{3} & 0 & +\frac{2}{3} & 0 & 0 \\ 0 & +\frac{1}{3} & +\frac{1}{3} & +\frac{1}{3} & 0 \\ 0 & 0 & +\frac{2}{3} & 0 & +\frac{1}{3} \\ 0 & 0 & 0 & +\frac{1}{3} & +\frac{2}{3} \end{pmatrix} \end{array} , \tag{21}$$

whereas if T is a deep trap, so that if the process *reaches* state T it remains there from that time on, we have

$$\underline{\mathcal{P}}=\begin{array}{c} \\ \mathcal{s}_T \\ \mathcal{s}_1 \\ \mathcal{s}_2 \\ \mathcal{s}_3 \\ \mathcal{s}_4 \end{array}\begin{array}{c} \begin{array}{ccccc} \mathcal{s}_T & \mathcal{s}_1 & \mathcal{s}_2 & \mathcal{s}_3 & \mathcal{s}_4 \end{array} \\ \begin{pmatrix} 1 & 0 & 0 & 0 & 0 \\ +\frac{1}{3} & 0 & +\frac{2}{3} & 0 & 0 \\ 0 & +\frac{1}{3} & +\frac{1}{3} & +\frac{1}{3} & 0 \\ 0 & 0 & +\frac{2}{3} & 0 & +\frac{1}{3} \\ 0 & 0 & 0 & +\frac{1}{3} & +\frac{2}{3} \end{pmatrix} \end{array} . \tag{22}$$

In the theory of finite Markov processes, one classifies the accessible states by distinguishing between two types of sets, transient sets and ergodic sets. Transient sets are sets that, once left, are never *entered* again; ergodic sets, once entered, are never left again. Thus, if we regard (only) the centrosymmetric site T of the lattice diagrammed in Fig. 3 to be a deep trap, the site T comprises a (one-state) ergodic set and the sites $\mathcal{s}_1$, $\mathcal{s}_2$, $\mathcal{s}_3$, and $\mathcal{s}_4$ comprise the transient set. Overall, the set of sites $\mathcal{s}_T$, $\mathcal{s}_1$, $\mathcal{s}_2$, $\mathcal{s}_3$, and $\mathcal{s}_4$ comprise an absorbing Markov chain.

Returning now to the transition matrix $\underline{\mathcal{P}}$, one can reorganize the information in $\underline{\mathcal{P}}$ in terms of ergodic sets and transient sets. In particular, the ergodic sets are united as one block division of $\underline{\mathcal{P}}$ with the transient sets comprising the remaining blocks. Supposing there are $\mathcal{s}$ transient states and $\mathcal{r}-\mathcal{s}$ ergodic states, $\underline{\mathcal{P}}$ may then be written as

$$\underline{\mathcal{P}}=\begin{array}{c} \\ \mathcal{r}-\mathcal{s} \\ \mathcal{s} \end{array}\begin{array}{c} \begin{array}{cc} \mathcal{r}-\mathcal{s} & \mathcal{s} \end{array} \\ \begin{pmatrix} \underline{\mathcal{L}} & \underline{0} \\ \underline{\mathcal{R}} & \underline{\mathcal{Q}} \end{pmatrix} \end{array} . \tag{23}$$

The $(\mathcal{r}-\mathcal{s})\times\mathcal{s}$ submatrix $\underline{0}$ consists entirely of zeros. The $\mathcal{s}\times\mathcal{s}$ submatrix $\underline{\mathcal{Q}}$ codes the fate of the random walker as long as it remains in the transient states. The $\mathcal{s}\times(\mathcal{r}-\mathcal{s})$ submatrix $\underline{\mathcal{R}}$ describes transitions which carry the random walker from transient states to ergodic states. Finally, the $(\mathcal{r}-\mathcal{s})\times(\mathcal{r}-\mathcal{s})$ submatrix $\underline{\mathcal{L}}$ codes the fate of the random walker after it enters an ergodic set. In the deep-trap problem summarized by the transition matrix $\underline{\mathcal{P}}$, Eq. (22), we would then identify

$$\underline{\mathcal{L}}=(1) , \tag{24}$$

$$\underline{0}=(0\ 0\ 0\ 0) , \tag{25}$$

$$\underline{\mathcal{R}}=\begin{pmatrix} +\frac{1}{3} \\ 0 \\ 0 \\ 0 \end{pmatrix} , \tag{26}$$

and

$$\underline{\mathcal{Q}}=\begin{pmatrix} 0 & \frac{2}{3} & 0 & 0 \\ \frac{1}{3} & \frac{1}{3} & \frac{1}{3} & 0 \\ 0 & \frac{2}{3} & 0 & \frac{1}{3} \\ 0 & 0 & \frac{1}{3} & \frac{2}{3} \end{pmatrix} . \tag{27}$$

From the theory of Markov processes[9] we know that in any finite Markov chain, no matter where the walker starts, the probability that the process is in an ergodic state after n steps tends to unity as $n\to\infty$ (Theorem 3.1.1). Thus, powers of $\underline{\mathcal{Q}}$ in the above aggregated version of $\underline{\mathcal{P}}$ tends to $\underline{0}$ and consequently for any absorbing Markov chain, the matrix $\underline{\mathbb{1}}-\underline{\mathcal{Q}}$ has an inverse $\underline{\mathcal{N}}$ (Theorem 3.2.1 and Definition 3.2.2).

Now, let $\mathcal{n}_j$ be the function giving the total number of times that the walker is in the transient state $\mathcal{s}_j$ (Definition 3.2.3), where the totality of transient states is denoted $\mathcal{T}$. Let $\mathcal{t}$ be the function giving the number of steps (including the original position) in which the walker is in a transient state (Definition 3.3.4). Then

$$\mathcal{t}=\sum_{\mathcal{s}_j\in\mathcal{T}} \mathcal{n}_j . \tag{28}$$

The totality of mean values of n_j for a process starting in state $\mathcal{S}_i$ is just the inverse matrix $\underline{\mathcal{N}}$ (Theorem 3.2.4), i.e.,

$$\{\mathcal{M}_i[n_j]\}=\underline{\mathcal{N}} \text{ when } \mathcal{S}_i,\mathcal{S}_j\in\mathcal{T} , \tag{29}$$

and the totality of mean values of t for a process starting in state $\mathcal{S}_i$ is given by the row sums of $\underline{\mathcal{N}}$ (Theorem 3.3.5), i.e.,

$$\{\mathcal{M}_i[t]\}=\underline{\mathcal{N}}\underline{\xi} , \tag{30}$$

where $\underline{\xi}$ is the column vector,

$$\underline{\xi}=\begin{bmatrix}1\\1\\\vdots\\1\end{bmatrix} . \tag{31}$$

With the above definitions and theorems at our disposal we are now ready to make contact with the formulation presented in the preceding section (and in I and II). With the use of the deep trap problem summarized by the matrix equation (10) as an example, it is evident that the matrix $\underline{A}$, Eq. (11), and $\underline{\mathcal{Q}}$, Eq. (27), are related as follows:

$$\mathbb{1}-\underline{\mathcal{Q}}=\underline{A} . \tag{32}$$

Hence, the fundamental matrix $\underline{\mathcal{N}}$ of the theory of Markov processes is given by

$$\underline{\mathcal{N}}=(\mathbb{1}-\underline{\mathcal{Q}})^{-1}=\underline{A}^{-1} , \tag{33}$$

where, for the problem at hand (Fig. 3 with site $\mathcal{S}_T$ a deep trap),

$$\underline{\mathcal{N}}=\underline{A}^{-1}=\begin{array}{c} \\ \mathcal{S}_1\\ \mathcal{S}_2\\ \mathcal{S}_3\\ \mathcal{S}_4\end{array}\begin{array}{c}\begin{array}{cccc}\mathcal{S}_1 & \mathcal{S}_2 & \mathcal{S}_3 & \mathcal{S}_4\end{array}\\ \begin{bmatrix}3 & 6 & 3 & 3\\ 3 & 9 & \frac{9}{2} & \frac{9}{2}\\ 3 & 9 & 6 & 6\\ 3 & 9 & 6 & 9\end{bmatrix}\end{array} . \tag{34}$$

The interpretation of the elements and row sums of the matrix $\underline{\mathcal{N}}$ follows directly from the definitions and theorems cited earlier. For example, if a walker starts in state $\mathcal{S}_3$, then it will be in state $\mathcal{S}_3$ an average of six times. Further, the total number of times a diffusing particle starting in $\mathcal{S}_3$ will be in state $\mathcal{S}_1$, in state $\mathcal{S}_2$, in state $\mathcal{S}_3$, and in state $\mathcal{S}_4$, will be given by the row sum $3+9+6+6=24$. In terms of our earlier notation, $\langle n\rangle_3=24$.

The above discussion makes precise the relationship between the formulation of the reaction-diffusion problem based on a self-consistent coding of the fate of a random walker as it confronts a site of given symmetry (I, II, and Sec. II C) and the traditional theory of absorbing Markov processes based on the identification of a transition probability matrix $\underline{\mathcal{P}}$. It is seen that the correspondence is one to one, except for two practical details. Firstly, the collapse in the number of variables that one achieves by taking advantage of the symmetry of lattice sites (see Fig. 3) as mobilized in Sec. II C can be understood within the framework of the theory of Markov processes as equivalent to the procedure[9] called "lumping." In working through the example using the Markov chain approach, we implicitly assumed that lumping of states $\mathcal{S}_i$ had already been achieved. Secondly, in the formulation given in Sec. II C, we designated the average number of steps taken by a random walker from a deep trap to be zero, i.e., we set $\langle n\rangle_T=0$. In the Markov approach, the probability of taking a step from a deep trap (an ergodic set) to itself again is unity. Thus the (1,1) element in Eq. (10) is unity, and consequently the (1,1) element of $\mathbb{1}-\widehat{A}$ is zero, whereas in the Markov formulation the (1,1) element of $\underline{\mathcal{P}}$ is unity. Provided this different convention for that single element is kept in mind, however, the correspondence between the two approaches is exact.

F. Connections with graph theory

In this subsection we will display the relationship between the methods described in the preceding discussion and the recursion method for lattice graphs. As will be seen, the graphical theory provides great insight into the number of sites visited in a random walk from site $\mathcal{S}_i$ to $\mathcal{S}_j$ and, as a consequence, reveals the underlying theoretical reason why the direct Monte Carlo simulation of average walk lengths in reaction-diffusion problems on finite and infinite (periodic) lattices in d dimensions[4-6] is so time consuming.

In what follows, we shall draw upon the ideas laid down in the seminal review of Kasteleyn.[10] To assist the reader, we shall stay close to the notation used in Ref. 10; where changes of notation are needed to avoid confusion with earlier parts of this paper, they will be indicated as introduced in the text.

Let us consider, for definiteness, the lattice displayed in Fig. 3 and regard it to be a graph G comprised of a certain number of points. In Kasteleyn's notation these points would be labeled $\mathcal{S}_i$; here, we denote these points using the symbol $\mathcal{S}_i$, the site specification introduced in the previous discussions. Now, let $\omega_n(\mathcal{S}\to\mathcal{S}')$ define the number of n-step walks on the graph G from the point $\mathcal{S}$ to the point $\mathcal{S}'$. For a conventional graph, it is evident that

$$\omega_n(\mathcal{S}\to\mathcal{S}')=\sum_{\mathcal{S}''\in G}\omega_{n-1}(\mathcal{S}\to\mathcal{S}'')\omega_1(\mathcal{S}''\to\mathcal{S}') , \tag{35}$$

so that

$$\omega_2(\mathcal{S}\to\mathcal{S}')=\sum_{\mathcal{S}''}\omega_1(\mathcal{S}\to\mathcal{S}'')\omega_1(\mathcal{S}''\to\mathcal{S}') , \tag{36}$$

$$\omega_3(\mathcal{S}\to\mathcal{S}')=\sum_{\mathcal{S}''}\sum_{\mathcal{S}'''}\omega_1(\mathcal{S}\to\mathcal{S}'')\omega_1(\mathcal{S}''\to\mathcal{S}''')\omega_1(\mathcal{S}'''\to\mathcal{S}')\cdots . \tag{37}$$

Kasteleyn notes that the structure of these equations suggests the introduction of a matrix with individual elements $\omega_1(\mathcal{S}\to\mathcal{S}')$. Upon labeling the points $\mathcal{S}_i$ of the graph G, an $N\times N$ matrix is defined. The elements of this matrix in the Kasteleyn notation are denoted a_{ij}; here, we shall use the script letter a_{ij} and define

$$a_{ij}\equiv\omega_1(\mathcal{S}_i\to\mathcal{S}_j) , \tag{38}$$

such that

$$a_{ij}=\begin{cases}0 \text{ if } \mathcal{S}_i \text{ and } \mathcal{S}_j \text{ are } \textit{not} \text{ adjacent}\\ 1,2,3,\ldots \text{ if } \mathcal{S}_i \text{ and } \mathcal{S}_j \textit{ are} \text{ adjacent and}\\ \qquad \text{connected by } 1,2,3,\ldots \text{ lines}.\end{cases} \tag{39}$$

The resulting symmetric matrix is called the adjacency matrix of the graph G and is denoted as A or $A(G)$ in Ref. (10); in what follows, we shall use the script symbols $\underline{\mathscr{A}}$ or $\underline{\mathscr{A}}(G)$ to denote the adjacency matrix. Then, the number $\omega_n(\mathcal{S}_i \to \mathcal{S}_j)$ of n-step walks between points (sites) $\mathcal{S}_i$ and $\mathcal{S}_j$ is given by the (i,j)th element of the nth power of $\underline{\mathscr{A}}$, viz.,

$$\omega_n(\mathcal{S}_i \to \mathcal{S}_j)=(\underline{\mathscr{A}}^n)_{ij}\ . \tag{40}$$

Finally, the generating function $\Gamma^w(\mathcal{S}_i \to \mathcal{S}_j;z)$, where z is a counting variable, is given by

$$\Gamma^w(\mathcal{S}_i \to \mathcal{S}_j;z)=[(\underline{\mathbb{1}}-z\underline{\mathscr{A}})^{-1}]_{ij}=\frac{\det(\underline{\mathbb{1}}_{ji}-z\underline{\mathscr{A}}_{ji})}{\det(\underline{\mathbb{1}}-z\underline{\mathscr{A}})}\ . \tag{41}$$

Considering the particular graph G defined by Fig. 3, we now construct the adjacency matrix for the problem. In the formulation presented in this section, we took advantage of the symmetry properties of the lattice. Thus, instead of labeling the 16 sites of Fig. 3 individually, we coded all sites of the lattice having the same symmetry by a single variable; instead of 16 sites, we considered as distinct the sites labeled T, 1, 2, 3, and 4 in Fig. 3. The only consequence of this simplification is that the associated adjacency matrix $\underline{\mathscr{A}}(G)$ of the problem is no longer symmetric; it is

$$\underline{\mathscr{A}}=\begin{array}{c} \\ \mathcal{S}_T\\ \mathcal{S}_1\\ \mathcal{S}_2\\ \mathcal{S}_3\\ \mathcal{S}_4\end{array}\begin{array}{c}\begin{array}{ccccc}\mathcal{S}_T & \mathcal{S}_1 & \mathcal{S}_2 & \mathcal{S}_3 & \mathcal{S}_4\end{array}\\ \begin{bmatrix}\omega_1(\mathcal{S}_T\to\mathcal{S}_T) & \omega_1(\mathcal{S}_T\to\mathcal{S}_1) & \omega_1(\mathcal{S}_T\to\mathcal{S}_2) & \omega_1(\mathcal{S}_T\to\mathcal{S}_3) & \omega_1(\mathcal{S}_T\to\mathcal{S}_4)\\ \omega_1(\mathcal{S}_1\to\mathcal{S}_T) & \omega_1(\mathcal{S}_1\to\mathcal{S}_1) & \omega_1(\mathcal{S}_1\to\mathcal{S}_2) & \omega_1(\mathcal{S}_1\to\mathcal{S}_3) & \omega_1(\mathcal{S}_1\to\mathcal{S}_4)\\ \omega_1(\mathcal{S}_2\to\mathcal{S}_T) & \omega_1(\mathcal{S}_2\to\mathcal{S}_1) & \omega_1(\mathcal{S}_2\to\mathcal{S}_2) & \omega_1(\mathcal{S}_2\to\mathcal{S}_3) & \omega_1(\mathcal{S}_2\to\mathcal{S}_4)\\ \omega_1(\mathcal{S}_3\to\mathcal{S}_T) & \omega_1(\mathcal{S}_3\to\mathcal{S}_1) & \omega_1(\mathcal{S}_3\to\mathcal{S}_2) & \omega_1(\mathcal{S}_3\to\mathcal{S}_3) & \omega_1(\mathcal{S}_3\to\mathcal{S}_4)\\ \omega_1(\mathcal{S}_4\to\mathcal{S}_T) & \omega_1(\mathcal{S}_4\to\mathcal{S}_1) & \omega_1(\mathcal{S}_4\to\mathcal{S}_2) & \omega_1(\mathcal{S}_4\to\mathcal{S}_3) & \omega_1(\mathcal{S}_4\to\mathcal{S}_4)\end{bmatrix}\end{array}, \tag{42}$$

or, explicitly, for periodic (confining) boundary conditions and no bias (weights) on the motion of the walker,

$$\underline{\mathscr{A}}=\begin{array}{c} \\ \mathcal{S}_T\\ \mathcal{S}_1\\ \mathcal{S}_2\\ \mathcal{S}_3\\ \mathcal{S}_4\end{array}\begin{array}{c}\begin{array}{ccccc}\mathcal{S}_T & \mathcal{S}_1 & \mathcal{S}_2 & \mathcal{S}_3 & \mathcal{S}_4\end{array}\\ \begin{bmatrix}0&3&0&0&0\\1&0&2&0&0\\0&1&1&1&0\\0&0&2&0&1\\0&0&0&1&2\end{bmatrix}\end{array}\ . \tag{43}$$

It is seen at once, from the discussion presented in Sec. II E that

$$\underline{\mathscr{A}}=\nu\underline{\mathscr{P}}\ , \tag{44}$$

where, again, ν is the valency of the lattice considered (here, $\nu=3$). Furthermore, if we consider the case of a deep trap at the site $\mathcal{S}_T$ and consider only the nontrapping sites, the matrix corresponding to $\underline{\mathscr{Q}}$ is

$$\underline{\mathscr{A}}(T)=\begin{bmatrix}0&2&0&0\\1&1&1&0\\0&2&0&1\\0&0&1&2\end{bmatrix}\ . \tag{45}$$

Since we know (Ref. 9, Theorem 3.2.1) that

$$\underline{\mathscr{N}}=(\underline{\mathbb{1}}-\underline{\mathscr{Q}})^{-1}=\underline{\mathbb{1}}+\underline{\mathscr{Q}}+\underline{\mathscr{Q}}^2+\cdots=\sum_{k=0}^{\infty}\underline{\mathscr{Q}}^k\ , \tag{46}$$

it is clear that, apart from the factor ν^{-k}, the construction of powers of $\underline{\mathscr{A}}(T)$, when summed to infinity, should yield the value of the (i,j)th element of the fundamental matrix $\underline{\mathscr{N}}$ of the theory of finite Markov processes. To demonstrate this relationship explicitly, we present in Fig. 7 the results obtained upon constructing the series

$$\underline{\mathscr{N}}=\underline{\mathbb{1}}+(1/\nu)\underline{\mathscr{A}}(T)+[(1/\nu)\underline{\mathscr{A}}(T)]^2+[(1/\nu)\underline{\mathscr{A}}(T)]^3+\cdots \tag{47}$$

for the lattice graph defined by Fig. 3 for periodic (confining) boundary conditions, equal *a priori* bias on the walks from site $\mathcal{S}_i \to \mathcal{S}_j$ and T a deep trap; in Fig. 8 calculations for representative elements of the fundamental matrix are presented for the next larger lattice, $N=25$. The asymptotes in Figs. 7(a)–7(d) equal the values listed in fundamental matrix $\underline{\mathscr{N}}$ for the problem $N=16$ listed in Sec. II E, viz., Eq. (34). Similar asymptotic results are obtained upon calculating Eq. (47) for the lattice graph corresponding to $N=25$, but with one important quantitative difference. Whereas for the lattice of size $N=16$, approximately 100 steps on the lattice are required to produce an estimate which is within 1% of the value given in Eq. (34), when one increases the fundamental unit lattice from $N=16$ to 25 many more steps are required to realize a comparable accuracy; in fact, approximately 100 steps on the $N=25$ lattice will bring one to within only 5% of the value for particular elements in the fundamental matrix $\underline{\mathscr{N}}$ for the problem.

The calculations summarized in Figs. 7 and 8 show in dramatic fashion why the direct Monte Carlo simulation of lattice walks is so time consuming. Even for the case of the smallest lattices (e.g., $N=16$ or 25 for $d=2$ hexagonal networks), hundreds of walks must be initiated from *each* site of the lattice in order to achieve the accuracy necessary for reliable estimates of the (i,j)th element of $\underline{\mathscr{N}}$, $\langle n\rangle_i$, and $\langle n\rangle$. For example, to obtain good histograms for the case of a $5\times5\times5$ cubic lattice with a centrosymmetric deep trap and values of $s=0.1$ characteriz-

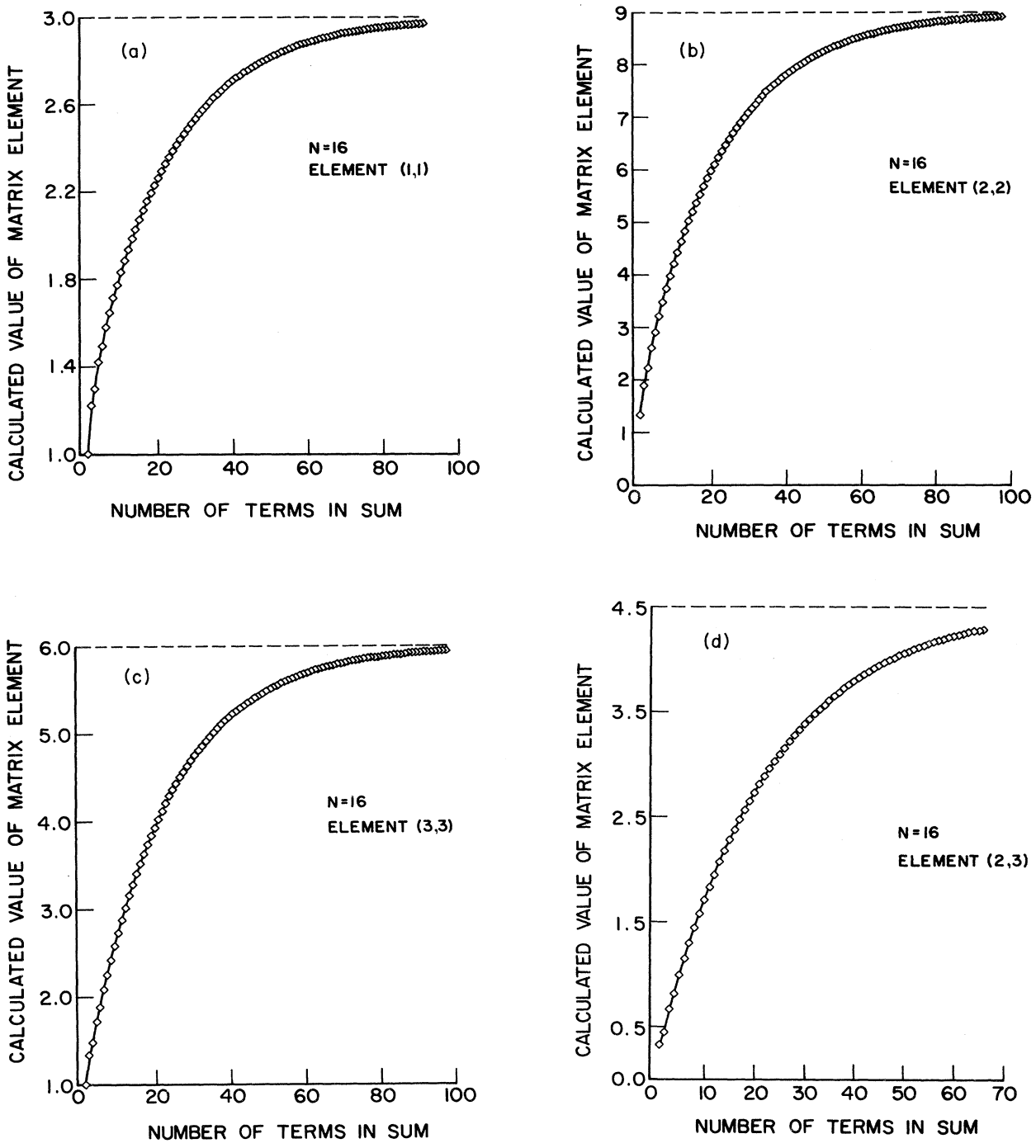

FIG. 7. Calculated value of the (i,j)th element of the fundamental matrix $\mathcal{M}$ for the $d=2$ hexagonal lattice with $N=16$ as a function of the number of terms considered in the sum, Eq. (47): (a) (1,1) element, (b) (2,2) element, (c) (3,3) element, and (d) (2,3) element. Dashed horizontal line in each case denotes the exact value of the element being calculated.

ing the possible absorption of the walker at the remaining $N-1$ sites of a periodic lattice, approximately 10 000 walkers from *each* of the $N-1$ sites of the lattice were necessary in the Monte Carlo simulation, a numerical experiment that consumed over 3 h of CPU time; direct calculation of the $\langle n \rangle_i$ and $\langle n \rangle$ based on the methods presented in Sec. II C required less than 3 sec on the same machine (IBM 370 computer).

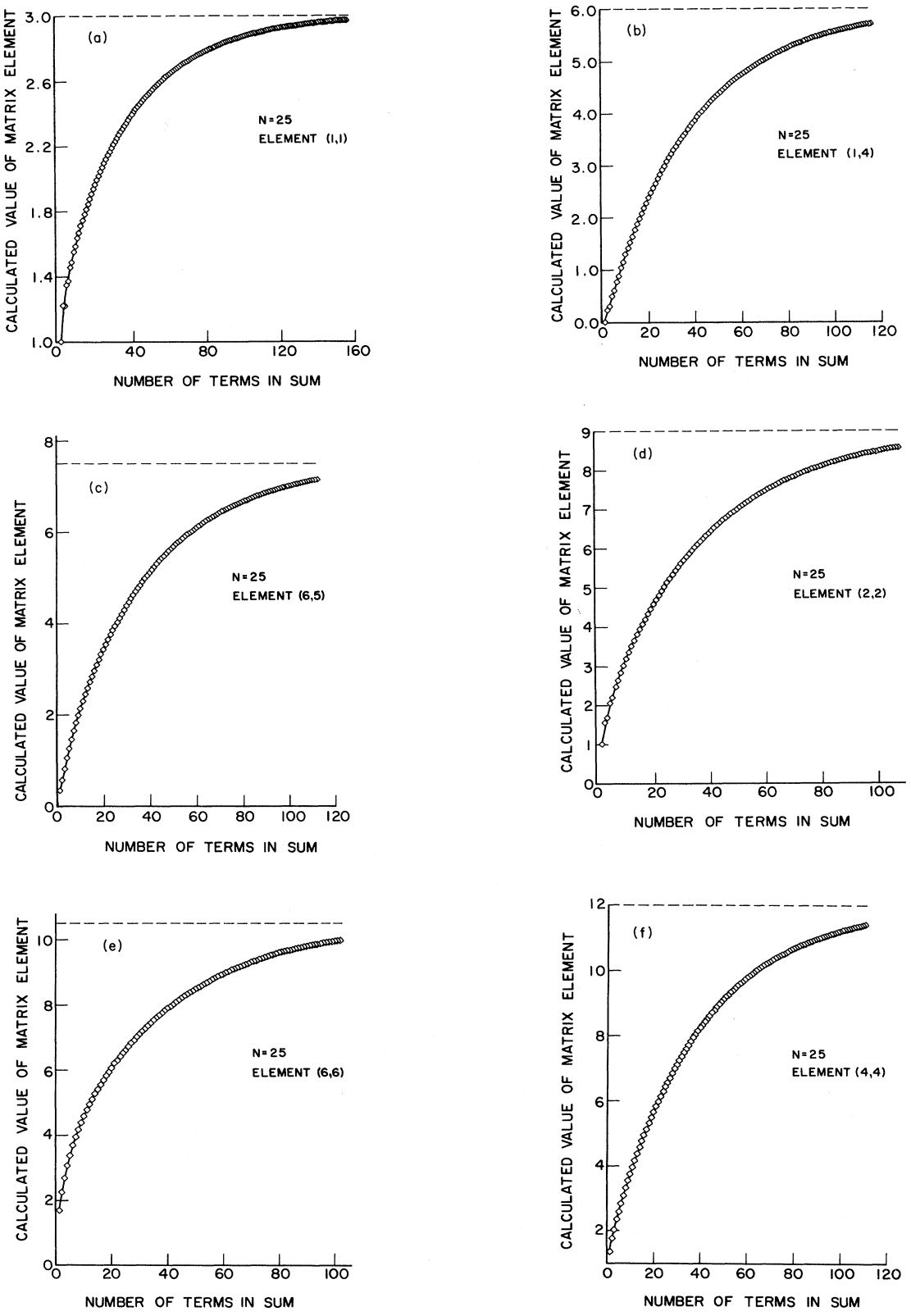

FIG. 8. Calculated value for the (i,j)th element of the fundamental matrix $\mathcal{N}$ for the $d=2$ hexagonal lattice with $N=25$ as a function of the number of terms considered in the sum, Eq. (47): (a) (1,1) element, (b) (1,4) element, (c) (6,5) element, (d) (2,2) element, (e) (6,6) element, and (f) (4,4) element. Dashed horizontal line in each case denotes the exact value of the element being calculated.

TABLE I. Results for $d=2$ hexagonal lattices subject to periodic or confining boundary conditions with a centrosymmetric deep trap ($p_T=1$) and with no background absorption (all $s_i=0$). Entries a–k are numbers calculated using Montroll's result, Ref. (1). The result of Monte Carlo simulation for $N=16$ is $\langle n \rangle = 21.62$ and for $N=25$ is $\langle n \rangle = 37.53$ (20 000 walkers per site).

N	16	49	100	169	256	361	25	64	121	196	289
$\langle n \rangle$	21.6[a]	86.6[b]	204.9[c]	381.8[d]	621.4[e]	926.8[f]	37.5[g]	119.6[h]	257.0[i]	454.4[j]	715.6[k]
$\langle n \rangle_1$	15.0	48.0	99.0	168.0	255.0	360.0	24.0	63.0	120.0	195.0	288.0
$\langle n \rangle_2$	21.0	70.5	147.0	250.5	381.0	538.5	34.5	93.0	178.5	291.0	430.5
$\langle n \rangle_3$	24.0	78.0	162.1	276.0	419.8	593.4	36.0	101.0	195.5	319.7	473.6
$\langle n \rangle_4$	27.0	90.0	189.2	324.1	494.5	700.3	40.5	112.0	217.0	355.3	526.9
$\langle n \rangle_5$		84.0	185.1	321.0	492.0	698.2	43.5	119.0	230.2	377.0	559.2
$\langle n \rangle_6$		82.5	176.9	304.5	465.2	659.1	46.5	130.0	253.7	417.4	620.8
$\langle n \rangle_7$		90.0	195.7	338.9	519.5	737.5		114.0	226.5	374.1	556.8
$\langle n \rangle_8$		94.5	201.3	346.7	530.4	752.3		119.0	240.5	399.8	596.9
$\langle n \rangle_9$		100.5	216.0	374.1	574.1	816.1		121.0	239.2	394.9	588.0
$\langle n \rangle_{10}$		103.5	222.4	385.1	591.2	840.6		129.0	257.2	426.7	637.2
$\langle n \rangle_{11}$		106.5	232.2	404.1	622.3	886.8		134.0	263.9	436.1	650.1
$\langle n \rangle_{12}$			198.4	351.0	542.6	773.4		140.0	277.9	461.1	689.4
$\langle n \rangle_{13}$			203.6	364.5	566.4	809.6		143.0	284.2	471.6	705.3
$\langle n \rangle_{14}$			205.8	362.5	559.9	798.1		146.0	293.7	489.6	734.3
$\langle n \rangle_{15}$			215.1	381.1	590.8	844.1			254.3	435.3	658.3
$\langle n \rangle_{16}$			221.4	387.4	597.8	852.3			252.8	427.3	642.9
$\langle n \rangle_{17}$			230.0	404.1	625.5	893.6			260.6	443.9	670.5
$\langle n \rangle_{18}$			235.6	412.1	636.4	908.3			265.5	446.1	670.4
$\langle n \rangle_{19}$			241.6	425.1	658.4	941.6			275.5	464.8	700.6
$\langle n \rangle_{20}$			244.6	431.2	668.3	956.1			282.6	472.6	709.7
$\langle n \rangle_{21}$			247.6	440.5	685.0	982.0			291.3	488.9	736.0
$\langle n \rangle_{22}$				378.6	601.8	869.5			297.0	497.2	747.2
$\langle n \rangle_{23}$				377.1	593.8	854.2			303.0	509.9	768.4
$\langle n \rangle_{24}$				385.2	610.1	880.7			306.0	516.0	778.1
$\langle n \rangle_{25}$				390.3	611.8	879.1			309.0	525.2	794.4
$\langle n \rangle_{26}$				401.6	631.4	909.4				448.2	686.1
$\langle n \rangle_{27}$				409.8	639.2	917.3				453.2	698.4
$\langle n \rangle_{28}$				420.9	657.9	945.8				455.2	695.2
$\langle n \rangle_{29}$				428.9	667.5	957.4				465.4	713.7
$\langle n \rangle_{30}$				437.8	683.3	981.9				472.7	718.7
$\langle n \rangle_{31}$				443.6	691.9	993.4				484.9	738.8
$\langle n \rangle_{32}$				449.6	704.3	1013.4				494.0	748.2
$\langle n \rangle_{33}$				452.6	710.4	1022.8				505.3	766.7
$\langle n \rangle_{34}$				455.6	719.5	1038.7				513.5	776.8
$\langle n \rangle_{35}$					614.8	896.9				522.4	792.5
$\langle n \rangle_{36}$					619.8	909.1				528.3	801.1
$\langle n \rangle_{37}$					621.8	905.7				534.3	813.5
$\langle n \rangle_{38}$					632.4	924.2				537.3	819.5
$\langle n \rangle_{39}$					640.1	928.9				540.3	828.6
$\langle n \rangle_{40}$					653.5	950.0					712.5
$\langle n \rangle_{41}$					663.8	959.7					711.0
$\langle n \rangle_{42}$					677.2	980.3					719.1
$\langle n \rangle_{43}$					687.5	991.8					724.2
$\langle n \rangle_{44}$					699.1	1010.1					736.8
$\langle n \rangle_{45}$					707.7	1021.0					746.5
$\langle n \rangle_{46}$					716.6	1036.4					760.8
$\langle n \rangle_{47}$					722.6	1045.2					772.1
$\langle n \rangle_{48}$					728.6	1057.4					785.8
$\langle n \rangle_{49}$					731.6	1063.4					796.4
$\langle n \rangle_{50}$					734.6	1072.5					808.1
$\langle n \rangle_{51}$						923.3					816.8
$\langle n \rangle_{52}$						921.8					825.7
$\langle n \rangle_{53}$						930.0					831.7
$\langle n \rangle_{54}$						935.2					837.7
$\langle n \rangle_{55}$						948.3					840.7

TABLE I. (*Continued*).

N	16	49	100	169	256	361	25	64	121	196	289
$\langle n \rangle_{56}$						958.4					843.7
$\langle n \rangle_{57}$						973.9					
$\langle n \rangle_{58}$						986.4					
$\langle n \rangle_{59}$						1002.0					
$\langle n \rangle_{60}$						1014.7					
$\langle n \rangle_{61}$						1028.8					
$\langle n \rangle_{62}$						1040.0					
$\langle n \rangle_{63}$						1051.8					
$\langle n \rangle_{64}$						1060.6					
$\langle n \rangle_{65}$						1069.5					
$\langle n \rangle_{66}$						1075.5					
$\langle n \rangle_{67}$						1081.5					
$\langle n \rangle_{68}$						1084.5					
$\langle n \rangle_{69}$						1087.5					
[a]20.4						[g]36.1					
[b]83.5						[h]115.8					
[c]198.8						[i]249.8					
[d]371.6						[j]442.7					
[e]606.0						[k]698.4					
[f]905.2											

III. RESULTS

We present in this section the results of (exact) calculations performed to study two types of reaction-diffusion processes. In the first series, we consider a reactant migrating toward a target molecule in a space of d dimensions and reacting there irreversibly upon first encounter. That is, we consider the reaction $A+B \rightarrow C$, where A may be regarded as the diffusing molecule and B the coreactant positioned at the reactive site of the lattice considered. Secondly, we shall assume that the $N-1$ sites surrounding the target molecule B (at the reactive site) are *not* passive (nonabsorbing or neutral) but may, with nonzero probability s, react with the diffusing molecule to form an excited-state complex resulting in the irreversible removal of the diffusing reactant from the system. That is, we imagine the $N-1$ sites of the host lattice are also occupied by B molecules which may compete to a certain extent ($0 \leq s < 1$) with the coreactant positioned at the active site; here we write, $A+B \rightleftarrows [AB]^* \rightarrow C$, where $[AB]^*$ is understood to be an intermediate activated complex.

We shall examine the efficiency of reaction in each of the above cases, as monitored by the quantities $\langle n \rangle_i$ and $\langle n \rangle$, as functions of the spatial extent of the system and of the boundary conditions imposed on the underlying lattice. In the following section, by comparing the results obtained here for hexagonal lattices with those obtained in our earlier work on square and/or cubic lattices, definite (quantitative) conclusions will be drawn on the role of lattice valency (and dimensionality) in influencing the efficiency of reaction-diffusion processes.

In Table I are presented the data on $\langle n \rangle_i$ and $\langle n \rangle$ for hexagonal lattices in $d=2$ subject to periodic or nontransmitting (confining) boundary conditions with a centrosymmetric deep trap ($p_T=1$) and no background absorption (i.e., we set the probability s_i of absorption at the $N-1$ background sites to zero). The results laid down in this table are to be taken in conjunction with Figs. 5(a) and 5(b) which display the symmetry and site classifications for the $d=2$ lattices considered. Taking together the data given in Table I with the locations of the sites $\mathcal{S}_i$ displayed in Figs. 5(a) and 5(b), one obtains a very detailed picture of the interplay between system geometry and reaction efficiency for the class of reactions considered here. Also indicated in this table are results calculated using the asymptotic formula[1] for $d=2$ hexagonal lattices subject to periodic boundary conditions and results calculated via our direct Monte Carlo simulation for the cases $N=16$ and 25. The latter (very time consuming) calculations yield the values $\langle n \rangle = 21.62$ and 37.53, respectively, results which are in excellent accord with the results obtained using the (exact) theory presented in Sec. II. From the discussion and results presented in Sec. II on these same lattice systems, we should expect to find that Monte Carlo calculations on hexagonal systems for $N > 25$ rapidly become impractical, and we do.

In Table II we consider the consequences of assuming that the background sites can, with a certain probability, react with the diffusing molecule A. Setting $s_i \neq 0$ for the $N-1$ sites surrounding the deep trap ($p_T=1$), one envisions the situation where at *any* one of the neighboring sites the molecule A may form an activated complex $[AB]^*$ with a resident B molecule, which may either fall apart (regenerating the molecule A) or react irreversibly with A to form the product C (i.e., $[AB]^* \rightarrow C$). The data displayed in Table II show that the "turning on" of reac-

TABLE II. Results for $d=2$ hexagonal lattices subject to periodic or confining boundary conditions with a centrosymmetric deep trap ($p_T=1$) and with background absorption ($s_i\neq 0$).

N	16	25	49	64	100	121	169	196	256	289	361
s	$\langle n\rangle$	$\langle n\rangle$	$\langle n\rangle$	$\langle n\rangle$	$\langle n\rangle$	$\langle n\rangle$	$\langle n\rangle$	$\langle n\rangle$	$\langle n\rangle$	$\langle n\rangle$	$\langle n\rangle$
0.00	21.60	37.50	86.62	119.62	204.86	256.96	381.79	454.41	621.38	715.64	926.77
0.05	10.47	13.05	16.12	16.98	18.04	18.38	18.84	19.00	19.23	19.32	19.46
0.10	6.93	7.92	8.92	9.17	9.47	9.56	9.69	9.73	9.79	9.82	9.85
0.15	5.18	5.69	6.17	6.29	6.43	6.47	6.52	6.54	6.57	6.58	6.60
0.20	4.14	4.45	4.72	4.79	4.86	4.89	4.92	4.93	4.95	4.95	4.96
0.25	3.45	3.65	3.82	3.87	3.91	3.93	3.95	3.96	3.97	3.97	3.98
0.30	2.96	3.10	3.21	3.24	3.28	3.29	3.30	3.30	3.31	3.31	3.32
0.35	2.59	2.69	2.77	2.79	2.82	2.82	2.83	2.84	2.84	2.84	2.85
0.40	2.31	2.38	2.44	2.45	2.47	2.48	2.48	2.48	2.49	2.49	2.49
0.45	2.08	2.13	2.18	2.19	2.20	2.20	2.21	2.21	2.21	2.21	2.22
0.50	1.89	1.93	1.97	1.97	1.98	1.99	1.99	1.99	1.99	1.99	2.00
0.60	1.60	1.63	1.65	1.65	1.66	1.66	1.66	1.66	1.66	1.66	1.66
0.70	1.39	1.41	1.42	1.42	1.42	1.42	1.43	1.43	1.43	1.43	1.43
0.80	1.23	1.24	1.24	1.25	1.25	1.25	1.25	1.25	1.25	1.25	1.25
0.90	1.10	1.11	1.11	1.11	1.11	1.11	1.11	1.11	1.11	1.11	1.11

tion centers at the $N-1$ sites surrounding the centrosymmetric deep trap has a dramatic effect on the efficiency of reaction in the diffusion-controlled process being considered. The average number $\langle n\rangle$ of steps required for trapping drops precipitously as s_i increases from zero. Indeed, only a 5% probability of reaction at the $N-1$ surrounding sites results in a drop in the value of $\langle n\rangle$ to a number approaching approximately 20 asymptotically as the system size increases. Beyond $N=100$, estimates of $\langle n\rangle$ for the setting of $s_i=0.05$ change by less than 1%, up to the largest lattices considered in this paper ($N=361$). In fact, as was demonstrated explicitly in II, $\langle n\rangle=1/s$ in the limit of an infinitely large system.

The results reported in Tables I and II pertain to periodic or nontransmitting boundary conditions. These boundary conditions may be regarded as passive in the sense that they do not seriously perturb the motion of the diffusing particle. However, situations where the boundary actively influences the diffusion process can also be studied using the methods laid down in Sec. II, and the results obtained in calculations of $\langle n\rangle_i$ and $\langle n\rangle$ for such problems are of great interest, given the avalanche of data on the kinetics of processes in compartmentalized systems[11] (micelles, vesicles, and microemulsions). Accordingly, we present results here for two classes of "active" boundary conditions. In Table III are listed results for $d=2$ hexagonal lattices subject to reflecting boundary conditions and assuming the equal-probability convention (see Sec. II B). The trap is taken to be a deep trap ($p_T=1$) and no background absorption (a set of competing reaction centers) is assumed. Then, in Table IV we examine the consequences of turning on the $N-1$ background sites, i.e., assuming a nonzero probability of reaction at each of these sites. A corresponding study of reaction efficiency for reflecting boundary conditions, but with the clockwise-bias convention assumed in governing the reinjection of the diffusing particle into the lattice, is presented in Tables V and VI.

The results presented in Tables III—VI, when compared against the earlier results reported for periodic or nontransmitting boundary conditions, Tables I and II, provide an explicit quantification of the anticipated "focusing effect" imparted by reflecting boundary conditions. The principal trends for the case of a passive background (all $s_i=0$) are conveniently displayed in Table VII. It is seen there that the results obtained using *either* convention for reflecting boundary conditions are essentially the same. Apparently, the biasing of the first step of the walker as it is reinjected into the lattice does not affect significantly the efficiency of reaction at the centrosymmetric site T. It is also evident, given the data reported in these tables, that the differences between periodic and nontransmitting (passive) and reflecting (active) boundary conditions becomes less and less the larger the size of the system studied. Since one anticipates that in the "thermodynamic limit" of the lattice statistical problem posed here that the boundaries should play *no* role in influencing the reaction-diffusion processes, this result is certainly sensible. It is interesting to note that the differences between results calculated using the two (passive versus active) classes of boundary conditions are already less than 10% for $N\geq 121$; apparently, a lattice of $N=121$ sites is already large enough that reaction at a centrosymmetric reaction center is not significantly perturbed by the boundary conditions imposed.

Also of interest is the extent to which *all* differences between lattices, both with respect to their size and with respect to the boundary conditions imposed, tend to become insignificant once competitive chemical processes are considered. As is seen in Tables II, IV, and VI,

TABLE III. Results for $d=2$ hexagonal lattices subject to reflecting boundary conditions (equal-probability convention) with a centrosymmetric deep trap ($p_T=1$) and with no background absorption (all $s_i=0$).

N	16	49	100	169	25	64	121	196
$\langle n \rangle$	15.2	72.5	181.9	349.2	28.8	102.7	230.8	418.5
$\langle n \rangle_1$	11.0	41.0	89.0	155.0	19.0	55.0	109.0	181.0
$\langle n \rangle_2$	15.0	60.0	132.0	231.0	27.0	81.0	162.0	270.0
$\langle n \rangle_3$	17.0	66.3	145.5	254.5	28.0	87.9	177.4	296.6
$\langle n \rangle_4$	18.0	75.9	169.4	298.5	31.0	97.1	196.6	329.4
$\langle n \rangle_5$		70.7	165.7	295.6	33.0	103.0	208.5	349.4
$\langle n \rangle_6$		69.7	158.5	280.5	34.0	111.8	229.2	386.4
$\langle n \rangle_7$		75.4	174.9	311.9		98.6	205.1	346.7
$\langle n \rangle_8$		79.1	179.9	319.0		102.5	217.5	370.3
$\langle n \rangle_9$		83.1	192.3	343.7		104.4	216.4	365.9
$\langle n \rangle_{10}$		85.1	197.7	353.5		110.5	232.1	394.9
$\langle n \rangle_{11}$		86.1	205.4	370.2		114.6	238.0	403.4
$\langle n \rangle_{12}$			177.0	322.8		118.6	249.8	425.9
$\langle n \rangle_{13}$			181.2	334.9		120.6	255.1	435.4
$\langle n \rangle_{14}$			183.3	333.1		121.6	262.6	451.2
$\langle n \rangle_{15}$			190.9	349.7			228.9	402.4
$\langle n \rangle_{16}$			196.4	355.5			227.9	395.3
$\langle n \rangle_{17}$			203.1	370.0			234.4	410.2
$\langle n \rangle_{18}$			207.7	377.1			238.9	412.3
$\langle n \rangle_{19}$			211.7	388.0			247.1	429.0
$\langle n \rangle_{20}$			213.7	393.1			253.3	436.1
$\langle n \rangle_{21}$			214.7	400.4			260.1	450.3
$\langle n \rangle_{22}$				346.7			264.8	457.6
$\langle n \rangle_{23}$				345.7			268.8	468.3
$\langle n \rangle_{24}$				352.6			270.8	473.4
$\langle n \rangle_{25}$				357.4			271.8	480.6
$\langle n \rangle_{26}$				367.0				413.6
$\langle n \rangle_{27}$				374.6				417.8
$\langle n \rangle_{28}$				383.7				419.9
$\langle n \rangle_{29}$				390.8				428.7
$\langle n \rangle_{30}$				397.6				435.5
$\langle n \rangle_{31}$				402.5				445.9
$\langle n \rangle_{32}$				406.5				454.2
$\langle n \rangle_{33}$				408.5				463.6
$\langle n \rangle_{34}$				409.5				470.9
$\langle n \rangle_{35}$								477.8
$\langle n \rangle_{36}$								482.7
$\langle n \rangle_{37}$								486.7
$\langle n \rangle_{38}$								488.7
$\langle n \rangle_{39}$								489.7

changes in a neutral background by only 5% result in a systematic collapse of results calculated for $\langle n \rangle$ to essentially similar values, almost irrespective of the factors cited above. These results can be used to provide quantitative estimates of the loss in efficiency of the energy-transfer process in the chlorophyll system in the specific situation where chlorophyll molecules comprising the antenna system may accidently trap the exciton as it moves to the preferred reaction center. Conversely, experimental data on catalyst deactivation can be correlated with the trends noted above, and the relative importance of different poisoning processes can be quantified. These two problems are planned to be treated in our subsequent work and the calculations will be presented elsewhere.

IV. DISCUSSION

In this paper we have examined several factors which may influence the efficiency of diffusion-controlled reactions and have quantified their relative importance using an exact lattice-statistical theory. We have considered the case where there exists a reactive center (B) towards which the diffusing molecule (A) migrates and reacts there, irreversibly, upon first encounter. We have also considered the case where the $N-1$ sites surrounding the (centrosymmetric) trap may compete with the centrally disposed reaction center, i.e., we have dealt with the case where a diffusing molecule can, with finite probability ($0 \leq s_i < 1$), react irreversibly with other molecules (B) po-

TABLE IV. Results for $d=2$ hexagonal lattices subject to reflecting boundary conditions (equal-probability convention) with a centrosymmetric deep trap ($p_T=1$) and with background absorption ($s_i\neq 0$).

N	16	25	49	64	100	121	169	196
s	$\langle n\rangle$	$\langle n\rangle$	$\langle n\rangle$	$\langle n\rangle$	$\langle n\rangle$	$\langle n\rangle$	$\langle n\rangle$	$\langle n\rangle$
0.00	15.20	28.75	72.50	102.67	181.87	230.85	349.17	418.45
0.05	8.89	12.02	15.74	16.75	17.95	18.32	18.81	18.98
0.10	6.28	7.60	8.83	9.12	9.45	9.55	9.68	9.73
0.15	4.85	5.56	6.14	6.27	6.43	6.47	6.52	6.54
0.20	3.96	4.38	4.71	4.78	4.86	4.89	4.92	4.93
0.25	3.34	3.61	3.82	3.86	3.91	3.93	3.95	3.96
0.30	2.89	3.07	3.21	3.24	3.28	3.29	3.30	3.30
0.35	2.54	2.68	2.77	2.79	2.82	2.82	2.83	2.84
0.40	2.27	2.37	2.44	2.45	2.47	2.48	2.48	2.48
0.45	2.06	2.13	2.18	2.19	2.20	2.20	2.21	2.21
0.50	1.88	1.93	1.97	1.97	1.98	1.99	1.99	1.99
0.60	1.60	1.63	1.65	1.65	1.66	1.66	1.66	1.66
0.70	1.39	1.41	1.42	1.42	1.42	1.42	1.43	1.43
0.80	1.23	1.24	1.24	1.25	1.25	1.25	1.25	1.25
0.90	1.10	1.11	1.11	1.11	1.11	1.11	1.11	1.11

TABLE V. Results for $d=2$ hexagonal lattices subject to reflecting boundary conditions (clockwise-bias convention) with a centrosymmetric deep trap ($p_T=1$) and with no background absorption (all $s_i=0$).

N	16	49	100	169	25	64	121	196
$\langle n\rangle$	15.2	72.2	181.0	347.5	28.7	102.2	229.8	416.5
$\langle n\rangle_1$	11.0	41.0	89.0	155.0	19.0	55.0	109.0	181.0
$\langle n\rangle_2$	16.0	60.3	132.2	231.2	27.4	81.3	162.2	270.1
$\langle n\rangle_3$	14.0	59.7	131.8	230.8	26.6	80.7	161.8	269.9
$\langle n\rangle_4$	17.0	66.2	145.4	254.4	28.1	88.0	177.5	296.7
$\langle n\rangle_5$	18.0	75.5	169.1	298.2	32.0	97.8	197.1	329.8
$\langle n\rangle_6$		71.2	166.0	295.9	29.7	96.2	196.0	328.9
$\langle n\rangle_7$		70.8	159.3	281.1	32.9	102.7	208.2	349.1
$\langle n\rangle_8$		68.8	158.0	280.1	33.9	111.0	228.5	385.8
$\langle n\rangle_9$		78.0	176.6	313.1		99.0	205.4	347.0
$\langle n\rangle_{10}$		72.6	173.2	310.6		104.9	219.1	371.6
$\langle n\rangle_{11}$		80.1	180.6	319.5		101.1	216.7	369.8
$\langle n\rangle_{12}$		77.2	178.3	317.7		106.4	217.9	367.0
$\langle n\rangle_{13}$		83.8	193.1	344.2		102.3	214.9	364.7
$\langle n\rangle_{14}$		80.5	189.6	341.3		113.4	234.4	396.7
$\langle n\rangle_{15}$		84.2	196.3	352.2		106.5	229.0	392.4
$\langle n\rangle_{16}$		85.2	203.2	368.1		115.4	238.7	403.9
$\langle n\rangle_{17}$			177.9	323.5		112.0	235.5	401.2
$\langle n\rangle_{18}$			184.9	337.5		118.9	250.3	426.3
$\langle n\rangle_{19}$			179.7	334.1		115.3	246.0	422.5
$\langle n\rangle_{20}$			186.9	335.8		119.1	252.9	433.3
$\langle n\rangle_{21}$			180.2	331.0		120.1	259.5	448.0
$\langle n\rangle_{22}$			196.2	353.8			230.7	403.8
$\langle n\rangle_{23}$			184.9	345.3			231.1	397.7
$\langle n\rangle_{24}$			199.4	358.0			226.8	394.6
$\langle n\rangle_{25}$			191.2	351.1			240.4	414.7
$\langle n\rangle_{26}$			205.8	372.8			230.1	407.3
$\langle n\rangle_{27}$			196.1	363.6			243.6	416.1
$\langle n\rangle_{28}$			207.5	377.0			233.7	408.4
$\langle n\rangle_{29}$			202.9	372.0			253.0	434.0
$\langle n\rangle_{30}$			210.5	387.1			239.0	422.5
$\langle n\rangle_{31}$			206.4	381.4			256.2	438.7

TABLE V. (*Continued*).

N	16	49	100	169	25	64	121	196
$\langle n\rangle_{32}$			210.5	388.8			246.6	430.0
$\langle n\rangle_{33}$			211.5	394.8			262.3	452.9
$\langle n\rangle_{34}$				349.4			251.7	442.0
$\langle n\rangle_{35}$				350.3			263.8	456.8
$\langle n\rangle_{36}$				344.8			258.9	451.0
$\langle n\rangle_{37}$				360.8			266.6	466.4
$\langle n\rangle_{38}$				347.8			262.4	460.1
$\langle n\rangle_{39}$				364.6			266.5	467.7
$\langle n\rangle_{40}$				350.9			267.5	473.6
$\langle n\rangle_{41}$				376.2				416.1
$\langle n\rangle_{42}$				356.4				424.5
$\langle n\rangle_{43}$				380.5				417.0
$\langle n\rangle_{44}$				364.6				427.2
$\langle n\rangle_{45}$				389.5				415.9
$\langle n\rangle_{46}$				370.9				439.5
$\langle n\rangle_{47}$				392.5				420.2
$\langle n\rangle_{48}$				380.3				444.1
$\langle n\rangle_{49}$				397.9				426.0
$\langle n\rangle_{50}$				385.8				455.8
$\langle n\rangle_{51}$				399.2				432.3
$\langle n\rangle_{52}$				393.6				460.2
$\langle n\rangle_{53}$				401.7				441.9
$\langle n\rangle_{54}$				397.2				468.9
$\langle n\rangle_{55}$				401.5				448.5
$\langle n\rangle_{56}$				402.5				471.7
$\langle n\rangle_{57}$								458.5
$\langle n\rangle_{58}$								476.9
$\langle n\rangle_{59}$								464.1
$\langle n\rangle_{60}$								478.0
$\langle n\rangle_{61}$								472.2
$\langle n\rangle_{62}$								480.4
$\langle n\rangle_{63}$								475.8
$\langle n\rangle_{64}$								480.1
$\langle n\rangle_{65}$								481.1

TABLE VI. Results for $d=2$ hexagonal lattices subject to reflecting boundary conditions (clockwise-bias convention) with a centrosymmetric deep trap ($p_T=1$) and with background absorption ($s_i\neq 0$).

N	16	25	49	64	100	121	169	196
s	$\langle n\rangle$	$\langle n\rangle$	$\langle n\rangle$	$\langle n\rangle$	$\langle n\rangle$	$\langle n\rangle$	$\langle n\rangle$	$\langle n\rangle$
0.00	15.20	28.70	72.20	102.25	181.03	229.78	347.50	416.47
0.05	8.89	12.02	15.73	16.74	17.95	18.32	18.81	18.98
0.10	6.28	7.60	8.83	9.12	9.45	9.55	9.68	9.73
0.15	4.85	5.56	6.14	6.27	6.42	6.47	6.52	6.54
0.20	3.96	4.38	4.71	4.78	4.86	4.89	4.92	4.93
0.25	3.34	3.61	3.82	3.86	3.91	3.93	3.95	3.96
0.30	2.89	3.07	3.21	3.24	3.28	3.29	3.30	3.30
0.35	2.54	2.68	2.77	2.79	2.82	2.82	2.83	2.84
0.40	2.27	2.37	2.44	2.45	2.47	2.48	2.48	2.48
0.45	2.06	2.13	2.18	2.19	2.20	2.20	2.21	2.21
0.50	1.88	1.93	1.97	1.97	1.98	1.99	1.99	1.99
0.60	1.60	1.63	1.65	1.65	1.66	1.66	1.66	1.66
0.70	1.39	1.41	1.42	1.42	1.42	1.42	1.43	1.43
0.80	1.23	1.24	1.24	1.25	1.25	1.25	1.25	1.25
0.90	1.10	1.11	1.11	1.11	1.11	1.11	1.11	1.11

TABLE VII. Comparison of results for $d=2$ hexagonal lattices subject to various boundary conditions and conventions with a centrosymmetric deep trap and with no background absorption (all $s_i \neq 0$).

N	$\langle n \rangle_{\text{PER}}$[a]	$\langle n \rangle_{R\text{-EPC}}$[b]	$\langle n \rangle_{R\text{-CBC}}$[c]	$\frac{\langle n \rangle_{\text{PER}} - \langle n \rangle_{R\text{-EPC}}}{\langle n \rangle_{\text{PER}}}$ (%)	$\frac{\langle n \rangle_{\text{PER}} - \langle n \rangle_{R\text{-CBC}}}{\langle n \rangle_{\text{PER}}}$ (%)
16	21.60	15.20	15.20	29.63	29.63
25	37.50	28.75	28.70	23.33	23.46
49	86.62	72.50	72.20	16.31	16.65
64	119.62	102.67	102.25	14.17	14.52
100	204.86	181.87	181.03	11.22	11.63
121	256.96	230.85	229.78	10.16	10.57
169	381.79	349.17	347.50	8.54	8.98
196	454.41	418.45	416.47	7.91	8.35

[a] $\langle n \rangle_{\text{PER}}$: Average walk length calculated assuming periodic boundary conditions.
[b] $\langle n \rangle_{R\text{-EPC}}$: Average walk length calculated assuming reflecting boundary conditions with the equal-probability convention.
[c] $\langle n \rangle_{\text{R-CBC}}$: Average walk length calculated assuming reflecting boundary conditions with the clockwise-bias convention.

sitioned at the $N-1$ sites. These studies were carried out specifically for hexagonal lattices in $d=2$ and 3 subject to several choices of finite-versus-infinite (periodic) boundary conditions, and data were presented for $\langle n \rangle_i$ and $\langle n \rangle$. Again $\langle n \rangle_i$ is the average (mean) number of steps required for a diffusing molecule to react starting from the site i and $\langle n \rangle$ represents the overall mean; these quantities reflect the efficiency of reaction on the lattices considered. Implicit in our calculations, though not presented in tables, were data on the number of times a diffusing particle, starting from site i, encounters a site j; these data are, of course, basic to the construction of the $\langle n \rangle_i$ (and $\langle n \rangle$). Rather, we displayed in Figs. 7 and 8, for the representative cases $N=16$ and 25, the number of steps required to achieve the exact value given by the theory of finite Markov processes. The data presented in these figures were compiled using the theory underlying the construction and manipulation of the adjacency-walk matrix for the problem. The insights gained in performing the latter calculations are twofold. Firstly, they demonstrate that graph theories designed to produce estimates of $\langle n \rangle_i$ (or $\langle n \rangle$) when based on only a few (less than 100) terms (walks and diagrams) are likely to be unsuccessful in reproducing the exact values reported in Tables I—VI. Secondly, these calculations show plainly why our earlier Monte Carlo numerical experiments were so time consuming; as indicated in Figs. 7 and 8, hundreds of walks from each site of the lattice are required to generate reliable (asymptotic) estimates of $\langle n \rangle$ for $N=16$ and 25, and from our earlier work[4–6] we can document that the situation deteriorates rapidly with further increase in the size of lattice unit.

The principal usefulness of the analysis presented in Sec. II is that interrelationships among three different approaches to the problem of diffusion-controlled reactions on d-dimensional lattices can be brought out and exploited. The algorithm (Sec. II C), reported in I and implemented in II, was deduced originally from a detailed study of the Monte Carlo results compiled on the general problem of random walks on finite and infinite lattices with traps.[4–6] The general theory of finite Markov processes turns out to be the underlying theoretical basis for the algorithm and in establishing this connection (Sec. II E) we now understand in terms of fundamental theorems why the algorithm "works" and works *exactly*. Finally, the graph theoretical and generating function approach to the same problem, as implemented in Sec. II F using the adjacency-walk matrix $\underline{\mathscr{A}}$, provides auxiliary information on and estimates of the number of steps required in individual site-to-site displacements on the lattice for the calculated statistical quantities to approximate the results encoded in the fundamental matrix $\underline{\mathscr{N}}$ of Markov chain theory. In effect, the numbers $\langle n \rangle_i$ calculated using the algorithm (or Markov chain theory) represent an adjacency-walk calculation in which an *infinite* number of such site-to-site steps are taken by the diffusing particle. In fact, if one associates a mean jump time with each step taken, the adjacency-walk calculations (as exemplified in Figs. 7 and 8) hint at the effective time scales required for equilibrium to be reached in diffusion-controlled reactions.

Given the data reported in our earlier study of square and cubic lattices (II) and the data on hexagonal lattices reported here, we can now consider in some detail the effects of lattice valency ν in influencing the efficiency of reaction-diffusion processes. Considering the $d=2$ case first, one anticipates that the smaller valency of the hexagonal lattice ($\nu=3$) as compared to the square lattice ($\nu=4$) might restrict the efficiency of reaction on hexagonal lattices simply because fewer paths to the reaction center are available to the diffusing particle. To quantify this, we report in Table VIII a comparison of results obtained for hexagonal versus square lattices for $d=2$ subject to periodic and nontransmitting boundary conditions with a centrosymmetric reaction center, a deep trap ($p_T=1$); we consider both neutral backgrounds (all $s_i=0$) and the case of $N-1$ competing reaction centers (with all $s_i=s\neq 0$). The usefulness of the classification scheme presented in Sec. II A can now be seen; because of the manner in which the basic simplex for the $d=2$ hexagonal lattice was constructed, hexagonal and square lattices characterized by the same overall value of N can be compared directly. From the data given in Table VIII, one

TABLE VIII. Comparison of $d=2$ results for hexagonal vs square lattices subject to periodic or confining boundary conditions with a centrosymmetric deep trap ($p_T=1$) and with background absorption ($s_i \neq 0$).

		$s_i=0.0$			$s_i=0.05$			$s_i=0.10$		
N	Square lattice	$\langle n \rangle_{sq}$	$\langle n \rangle_{hex}$	Percent difference	$\langle n \rangle_{sq}$	$\langle n \rangle_{hex}$	Percent difference	$\langle n \rangle_{sq}$	$\langle n \rangle_{hex}$	Percent difference
25	5×5	31.7 (31.6)[a]	37.5 (36.1)	18.3	12.4	13.0	5.3	7.71	7.92	2.7
49	7×7	71.6 (71.6)	86.6 (83.6)	21.0	15.6	16.1	3.1	8.79	8.92	1.5
121	11×11	209.9 (209.9)	257.0 (249.8)	22.4	18.2	18.4	1.2	9.51	9.56	0.53
169	13×13	310.6 (310.6)	381.8 (371.6)	22.9	18.7	18.8	0.86	9.65	9.69	0.41
289	17×17	579.4 (579.5)	715.6 (698.4)	23.5	19.2	19.3	0.47	9.80	9.82	0.20
361	19×19	748.9 (749.1)	926.8 (905.2)	23.8	19.4	19.5	0.41	9.84	9.85	0.10

[a]Numbers in parentheses are the Montroll asymptotic estimates of $\langle n \rangle$.

finds that the percent difference in values calculated for $\langle n \rangle$ in the two cases is approximately 18% for the smallest lattice considered ($N=25$) but increases only a further 6% when the largest lattices studied here ($N=361$) are compared. Although there is a persistent difference between the values of $\langle n \rangle$ calculated for hexagonal versus square lattices, this difference seems to approach asymptotically a value just under 25%. Once again it is worth drawing attention to the leveling effect produced when the $N-1$ surrounding sites are turned on chemically. When there is a nonzero probability that reaction may occur at the $N-1$ neighboring sites, the percent differences recorded in Table VIII between the two lattices *decrease* with increasing lattice size, an effect which becomes more pronounced the larger the value of the $s_i=s$. Even a 5% probability of reaction at these $N-1$ sites collapses the difference in calculated values of $\langle n \rangle$ for $\nu=3$ vs $\nu=4$ for $d=2$ to within a few percent.

As noted earlier, periodic boundary conditions imposed on a hexagonal or square lattice with a centrosymmetric trap are equivalent to nontransmitting (or confining) boundary conditions imposed on the same lattice. Hence the results reported in Table VIII are also of interest in considering reaction efficiencies for a finite cluster of sites subject to passive boundary conditions. Some consequences of permitting the boundary to influence in an active way the fate of a diffusing particle traversing a finite cluster of sites were explored earlier by considering reflecting boundary conditions. Whereas for the case of square lattices, the imposition of reflecting boundary conditions presented no ambiguities regarding the fate of the molecule as it reenters the lattice, the situation is otherwise for hexagonal lattices (Sec. II C). Accordingly for the hexagonal lattices studied here, two sorts of reflecting boundary conditions were designed and data were presented for the equal-probability convention and the clockwise-bias convention. In Table IX we present a comparison of the numbers $\langle n \rangle$ generated for $d=2$ for reflecting boundary conditions for square lattices ($\nu=4$) and for hexagonal lattices ($\nu=3$), the latter subject to the two conventions noted above. While the numbers $\langle n \rangle$ calculated for reflecting boundary conditions are different from those calculated for periodic and nontransmitting boundary conditions, it is also clear from Table IX that the principal trends noted earlier for periodic boundary conditions (Table VIII) pertain here as well. Again we see that once the chemical reactivity of the $N-1$ sites surrounding the centrosymmetric reaction center becomes a factor ($s=0.05$), differences in $\langle n \rangle$ for the *same* lattice subject to different boundary conditions or differences between lattices of different valencies but subject to the same boundary conditions tend to evaporate. In the language of

TABLE IX. Comparison of results for $d=2$ hexagonal vs square lattices subject to reflecting boundary conditions with a centrosymmetric deep trap ($p_T=1$) and with background absorption ($s_i \neq 0$).

		$s_i=0.00$			$s_i=0.05$			$s_i=0.10$		
N	Square lattice	$\langle n \rangle_{sq}$[a]	$\langle n \rangle_{EPC}$[b]	$\langle n \rangle_{CBC}$[b]	$\langle n \rangle_{sq}$	$\langle n \rangle_{EPC}$[b]	$\langle n \rangle_{CBC}$[b]	$\langle n \rangle_{sq}$	$\langle n \rangle_{EPC}$[b]	$\langle n \rangle_{CBC}$[b]
25	5×5	19.1	28.8	28.7	10.1[c]	12.0	12.0	6.88[c]	7.60	7.60
49	7×7	50.7	72.5	72.2	14.6[c]	15.7	15.7	8.54[c]	8.83	8.83
121	11×11	170.4	230.8	229.8	18.0	18.3	18.3	9.48	9.55	9.55
169	13×13	260.9	349.2	347.5	18.6	18.8	18.8	9.64	9.68	9.68

[a]Data taken from Ref. 8.
[b]Hexagonal-lattice walk-length data.
[c]C. A. Walsh (private communication).

TABLE X. Comparison of results for $d=3$ hexagonal vs cubic lattices subject to periodic boundary conditions with a centrosymmetric deep trap ($p_T=1$) and with background absorption ($s_i\neq 0$).

		$s=0.0$				$s=0.05$	
N	Cubic lattice	$\langle n\rangle_{\text{cubic}}$	$\langle n\rangle_{\text{hex}}$	$\langle n\rangle_{\text{MONTROLL}}$[a]	$\frac{\lvert\langle n\rangle_{\text{calc}}-\langle n\rangle_{\text{MONTROLL}}\rvert}{\langle n\rangle_{\text{MONTROLL}}}$ (%)[b]	$\langle n\rangle_{\text{cubic}}$	$\langle n\rangle_{\text{hex}}$
	Cubic						
27	$3\times3\times3$	30.46		42.16	27.8	12.27	
125	$5\times5\times5$	157.32		195.18 (157.3)	19.4	17.80	
343	$7\times7\times7$	455.27		535.56	15.0	19.17	
				Hexagonal			
55			77.27	85.88	10.0		15.92
91			131.59	142.09	7.4		17.37
285			443.37	444.99	0.36		19.12

[a]Montroll's asymptotic estimate for *cubic* lattices; $\langle n\rangle_{\text{MONTROLL}}\simeq 1.5614(N)$. Number in parentheses for the $5\times5\times5$ cubic lattice is the result obtained by refining Montroll's estimate [M. D. Hatlee (private communication)]. Corresponding Monte Carlo result for this case is $\langle n\rangle=157.5$.

[b]$\langle n\rangle_{\text{calc}}=\langle n\rangle_{\text{cubic}}$ *or* $\langle n\rangle_{\text{hex}}$.

Markov chain theory, introduction of (partial) ergodic character into the description of the transient states of the system permits them to become very effective competitors with the single, purely ergodic state of the problem (the deep trap).

Many of the studies reported above were repeated for the dimensionality $d=3$. The symmetry analysis (Sec. II A) and the specification of boundary conditions (Sec. II C) goes through for $d=3$ exactly as for $d=2$; here, three-dimensional models are invaluable in facilitating site classifications for different boundary conditions. Rather than present extensive banks of data here (these are available upon request), we simply record in Table X some representative comparison of cubic ($\nu=6$) versus hexagonal ($\nu=4$) lattices for $d=3$. For $d=3$ one loses an important simplifying feature of the $d=2$ comparisons; it is not possible (for a centrosymmetric trap and periodic boundary conditions) to construct cubic versus hexagonal lattices with the same overall N. Although exact correspondences are not possible, an examination of the data in Table X reveals that the trends identified earlier in the $d=2$ case persist here as well. Also listed in Table X are the differences between the exact numerical results calculated using the theory outlined in Sec. II D and the asymptotic results calculated using the Montroll theory. It is interesting, though accidental, that Montroll's estimate[1] for cubic lattices works better for hexagonal lattices for $d=3$ than for cubic ones.

The data presented in this work provide a storehouse of exact information which can be used to guide the development of analytic theories of random walks on d-dimensional lattices. For example, it had been known since the earlier, classic studies of Montroll and Weiss[1] that the mean number of steps required for trapping on a periodic lattice from a nearest-neighbor site to a centrosymmetric deep trap is given (in our notation) by[12] $\langle n\rangle_1=N-1$. The results displayed in Sec. III certainly confirm this and show further that the mean number of steps required for trapping on a hexagonal, periodic lattice from a *next*-nearest-neighbor site to a centrosymmetric deep trap is given by $\langle n\rangle_2=3[(N/2)-1]$, a result which follows at once from the above expression for $\langle n\rangle_1$ and Eq. (8). These analytic expressions for $\langle n\rangle_1$ and $\langle n\rangle_2$ in terms of N constitute invariance relations for the lattices specified above and, as was mentioned in II, can be used in conjunction with certain decimationlike transformations to produce analytic expressions for $\langle n\rangle$ in terms of the underlying variables of the problem (e.g., ν, d, and N). The decimationlike transformations introduced in II have, we believe, a direct counterpart in the theory of finite Markov processes and we hope to be able to demonstrate in our subsequent work how theorems on ergodic chains may be used to simplify the analysis of absorbing Markov chains (and vice versa).

Finally, we again draw attention to the fact that there exist several important physical problems for which it is recognized that the efficiency of the underlying process can be compromised by competitive trapping mechanisms. Principal among these are the problems of energy migration and trapping on chlorophyll networks and those of catalyst deactivation in partially poisoned supports. With the results presented in II and in the present study we now have at our disposal an extensive bank of data on the role of system size, dimensionality, boundary conditions, and lattice valency that can be used to guide the construction of models for these processes; we plan to report these studies in the near future.

ACKNOWLEDGMENTS

The research described herein was supported by the Office of Basic Energy Sciences of the U.S. Department of Energy. This is Document No. NDRL-2504 from the Notre Dame Radiation Laboratory. The authors would like to thank G. H. Weiss (National Institutes of Health) and G. F. Lawler (Duke University) for their help and suggestions.

[1]See, for example, the classic papers, E. W. Montroll, Proc. Symp. Appl. Math. Am. Math. Soc. 16, 193 (1964); E. W. Montroll and G. H. Weiss, J. Math. Phys. 6, 167 (1965); E. W. Montroll, J. Math. Phys. 10, 753 (1969).

[2]See the review article by G. H. Weiss and R. J. Rubin, Adv. Chem. Phys. 52, 363 (1982), and references therein.

[3]See the proceedings of the conference, Symposium on Random Walks and Their Application to the Physical and Biological Sciences [J. Stat. Phys. 30, 263 (1983)].

[4]M. D. Hatlee and J. J. Kozak, Phys. Rev. B 21, 1400 (1980).

[5]M. D. Hatlee and J. J. Kozak, Phys. Rev. B 23, 1713 (1981).

[6]M. D. Hatlee and J. J. Kozak, Proc. Nat. Acad. Sci. U.S.A. 78, 972 (1981).

[7]C. A. Walsh and J. J. Kozak, Phys. Rev. Lett. 47, 1500 (1981).

[8]C. A. Walsh and J. J. Kozak, Phys. Rev. B 26, 4166 (1982).

[9]J. G. Kemeny and J. L. Snell, *Finite Markov Chains* (Van Nostrand, Princeton, New Jersey, 1960).

[10]P. W. Kasteleyn, in *Graph Theory and Theoretical Physics*, edited by F. Harary (Academic, New York, 1967), p. 44.

[11]C. Tanford, *The Hydrophobic Effect* (Wiley, New York, 1973); J. H. Fendler and E. J. Fendler, *Catalysis in Micellar and Macromolecular Systems* (Academic, New York, 1975); J. K. Thomas, Acc. Chem. Res. 10, 133 (1977).

[12]The result $\langle n \rangle_1 = N-1$ can be derived simply as follows: Let $\langle n \rangle_x$ be the expected number of steps to the trap, denoted by 0; $\langle n \rangle_0 = 0$. $x \sim y$ means that x and y are connected by a bond on the lattice, and ν is the valency of the lattice G. Then,

$$\sum_{x \in G} \langle n \rangle_x = \sum_{\substack{x \in G, \\ x \neq 0}} \sum_{x \sim y} \frac{1}{\nu} (\langle n \rangle_y + 1)$$

$$= \left[\sum_{x \in G} \langle n \rangle_x \right] + (N-1) - \frac{1}{\nu} \sum_{y \sim 0} \langle n \rangle_y ,$$

from which the Montroll-Weiss result follows at once.